

SHIELDING EFFECTIVENESS OF A THIN FILM WINDOW

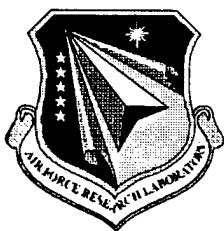
Lt Eric Johnson
Lt Wesley Turner

April 1998

Final Report

19980615 045

APPROVED FOR PUBLIC RELEASE; DISTRIBUTION IS UNLIMITED.



AIR FORCE RESEARCH LABORATORY
Directed Energy Directorate/ DEPE
3550 Aberdeen Ave SE
AIR FORCE MATERIEL COMMAND
KIRTLAND AIR FORCE BASE, NM 87117-5776

AFRL-DE-PS-TR-1998-1034

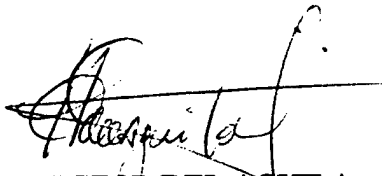
Using Government drawings, specifications, or other data included in this document for any purpose other than Government procurement does not in any way obligate the U.S. Government. The fact that the Government formulated or supplied the drawings, specifications, or other data, does not license the holder or any other person or corporation; or convey any rights or permission to manufacture, use, or sell any patented invention that may relate to them.

This report has been reviewed by the Public Affairs Office and is releasable to the National Technical Information Service (NTIS). At NTIS, it will be available to the general public, including foreign nationals.

If you change your address, wish to be removed from this mailing list, or your organization no longer employs the addressee, please notify AFRL/DEPE, 3550 Aberdeen Ave SE, Kirtland AFB, NM 87117-5776.

Do not return copies of this report unless contractual obligations or notice on a specific document requires its return.

This report has been approved for publication.

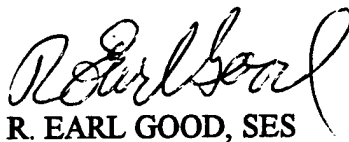


HECTOR DEL AGUILA
Project Manager

FOR THE COMMANDER



JORGE E. BERAUN, DR-IV
Chief, DE Effects Research Branch



R. EARL GOOD, SES
Director, Directed Energy Directorate

REPORT DOCUMENTATION PAGE			Form Approved OMB No. 0704-0188	
<small>Public reporting burden for this collection of information is estimated to average 1 hour per response, including the time for reviewing instructions, searching existing data sources, gathering and maintaining the data needed, and completing and reviewing the collection of information. Send comments regarding this burden estimate or any other aspect of this collection of information, including suggestions for reducing this burden, to Washington Headquarters Services, Directorate for Information Operations and Reports, 1215 Jefferson Davis Highway, Suite 1204, Arlington, VA 22202-4302, and to the Office of Management and Budget, Paperwork Reduction Project (0704-0188), Washington, DC 20503.</small>				
1. AGENCY USE ONLY (Leave blank)		2. REPORT DATE April 1998		3. REPORT TYPE AND DATES COVERED Final; September 1997 - February 1998
4. TITLE AND SUBTITLE Shielding Effectiveness of a Thin Film Window			5. FUNDING NUMBERS PE: 62601F PR: 5797 TA: AL WU: 04	
6. AUTHOR(S) Eric Johnson and Wesley Turner				
7. PERFORMING ORGANIZATION NAME(S) AND ADDRESS(ES) Air Force Research Laboratory/DEP 3550 Aberdeen Ave SE Kirtland AFB, NM 87117-5776			8. PERFORMING ORGANIZATION REPORT NUMBER AFRL-DE-PS-TR-1998-1034	
9. SPONSORING/MONITORING AGENCY NAME(S) AND ADDRESS(ES)			10. SPONSORING/MONITORING AGENCY REPORT NUMBER	
11. SUPPLEMENTARY NOTES				
12a. DISTRIBUTION AVAILABILITY STATEMENT Approved for public release; distribution is unlimited.			12b. DISTRIBUTION CODE	
13. ABSTRACT (Maximum 200 words) <p>The thin film investigated was designed to protect infra-red (IR) systems from electromagnetic interference (EMI), yet allow IR to pass through the thin film window. This experiment measured the properties of a thin film developed by Sienna Technologies, Inc., through a Phase II Small Business Innovative Research (SBIR) program. The objectives of this SBIR were to shield the system from EMI by at least 20 dB from 400 MHz to 18 GHz, and transmit at least 90% of the IR around 1 um and between 8 - 12 um.</p> <p>The measured shielding effectiveness of the thin film was 25 dB from 4 GHz to 12 GHz. The predicted shielding effectiveness was 29 dB based on theoretical calculations. The error analysis of the shielding effectiveness showed that this predicted value was within the measurement error of the experiment. The shielding effectiveness of the substrate was also measured, and it did not contribute to the shielding effectiveness of the thin film. Shielding effectiveness was measured in an electronically mode-stirred reverberation chamber to get a quick overview and in an anechoic chamber to measure the shielding effectiveness versus incident angle. The IR transmission of the thin film could not be determined because of the low IR transmission through the substrate.</p>				
14. SUBJECT TERMS Electrically conductive metal silicide, Electromagnetic interference, High Power Microwaves, Radio Frequency, Hardening, Coupling, Infrared, meshes, transmittance			15. NUMBER OF PAGES 70	
			16. PRICE CODE	
17. SECURITY CLASSIFICATION OF REPORT Unclassified	18. SECURITY CLASSIFICATION OF THIS PAGE Unclassified	19. SECURITY CLASSIFICATION OF ABSTRACT Unclassified	20. LIMITATION OF ABSTRACT Unl	

EXECUTIVE SUMMARY

The thin film investigated was designed to protect infra-red (IR) systems from electromagnetic interference (EMI), yet allow IR to pass through the thin film window. This experiment measured the properties of a thin film developed by Sienna Technologies, Inc., through a Phase II Small Business Innovative Research (SBIR) program. The objectives of this SBIR were to shield the system from EMI by at least 20 dB from 400 MHz to 18 GHz, and transmit at least 90% of the IR around 1 μm and between 8 – 12 μm .

The measured shielding effectiveness of the thin film was 25 dB from 4 GHz to 12 GHz. The predicted shielding effectiveness was 29 dB based on theoretical calculations. The error analysis of the shielding effectiveness showed that this predicted value was within the measurement error of the experiment. The shielding effectiveness of the substrate was also measured, and it did not contribute to the shielding effectiveness of the thin film. Shielding effectiveness was measured in an electronically mode-stirred reverberation chamber to get a quick overview and in an anechoic chamber to measure the shielding effectiveness versus incident angle.

The IR transmission could not be determined because of the low IR transmission through the substrate. (The thin film was sputtered onto the substrate.) A different yet still inexpensive substrate will be used in the future, so the IR transmission can be measured. A zinc-sulfide substrate will be used in the final thin film window, but it is too expensive to use for research purposes. The IR transmission of the thin film was never previously measured, so there was no prediction for it. Research showed that the thin film material selected could transmit up to 90% IR [6], and IR measurements of similar materials showed that a transmission of 60 - 70% should be expected [2].

ACKNOWLEDGMENTS

We would like to thank Dr. Ender Savrun and Dr. Cetin Toy of Sienna Technologies, and Mr. Hector Del Aguila, Maj. Thomas Loughry, Mr. Kerry Sandstrom, Capt. John Allison, and Dr. Jane Lehr of the Air Force Research Laboratory for help with developing this report.

TABLE OF CONTENTS

EXECUTIVE SUMMARY.....	iii
ACKNOWLEDGMENTS	iv
TABLE OF CONTENTS	v
LIST OF ILLUSTRATIONS	vii
List of Tables.....	vii
List of Figures	vii
ABBREVIATIONS	viii
DEFINITIONS	ix
1.0 Introduction.....	1
1.1 Historical Background of this Small Business Innovative Research	1
1.2 Purpose	3
1.3 Objectives.....	3
1.4 Overview	3
2.0 Theoretical Background.....	4
2.1 Predicted Shielding Effectiveness of Thin Film Windows.....	4
2.2 Isolation between the Reverberation Chamber and the Nested Chamber.....	8
2.3 Lower Operating Frequency of the Nested Chamber.....	9
2.4 IR Transmission	10
3.0 Experimental Setup.....	11
3.1 Materials Tested	11
3.2 Reverberation Chamber Experimental Setup	12
3.3 Band-Limited White-Gaussian Noise Experimental Setup	13
3.4 Continuous Wave Anechoic Chamber Experimental Setup	14
3.5 Antennas Used.....	15
3.6 Laser Measurements	16
4.0 Measurement Results	17
4.1 Shielding Effectiveness Measurements.....	17
4.2 Measured Losses.....	24
4.3 Isolation Measurements	25

4.4	Field Uniformity Measurements and Lower Operating Frequency.....	26
4.5	Error Analysis for Shielding Effectiveness Measurements	29
4.6	IR Transmission Measurements	32
5.0	Conclusions.....	34
6.0	Recommendations	35
7.0	References	36
	Appendix A: Graphs	37

LIST OF ILLUSTRATIONS

List of Tables

Table 1: Calculated Skin Depths for Different Windows	4
Table 2: Predicted Shielding Effectiveness Due to Absorption and Reflection	8
Table 3: Minimum Operating Frequency for Nested Chamber	10

List of Figures

Figure 1. Predicted Shielding Effectiveness vs. Frequency for a Thin and Thick Film.....	7
Figure 2. Predicted Shielding Effectiveness vs. Thickness for 9.2 Ω /square	7
Figure 3: EMSC Experimental Setup	13
Figure 4: BLWGN Experimental Setup.....	14
Figure 5: CW Experimental Setup	15
Figure 6: Shielding Effectiveness of the Thin Film Using the EMSC.....	18
Figure 7: Shielding Effectiveness of the Polished Substrate Using the EMSC	19
Figure 8: Overlay of the Open Aperture, Thin Film, and Closed Aperture.....	20
Figure 9: Shielding Effectiveness of the Thin Film at 0° Incidence Using BLWGN	21
Figure 10: Overlay of the Open Aperture, Thin Film, and Closed Aperture Measurements at 0° Incidence Using BLWGN	21
Figure 11: Attempted CW Measurement	22
Figure 12: Comparison of the EMSC and BLWGN SE Measurements	23
Figure 13: Isolation Provided by the Nested Chamber Aperture.....	25
Figure 14: Field Uniformity in the Large Chamber Using a 50 and 100 MHz NBW	26
Figure 15: Field Uniformity in the Nested Chamber Using a 50 and 100 MHz NBW	27
Figure 16: Error Between 2 Probes in the BLWGN Nested Chamber with 100 MHz.....	28
Figure 17: Wave Impedance in a Reverberation Chamber	31
Figure 18. IR Transmission Measurements.....	32

ABBREVIATIONS

<u>Abbreviation</u>	<u>Definition</u>
---------------------	-------------------

AFRL	Air Force Research Laboratory
AlN	Aluminum Nitride
BLWGN	Band-Limited White-Gaussian Noise
DE	Directed Energy Directorate
DEPE	Effects Research Branch
DUT	Device Under Test
EMI	Electromagnetic Interference
EMSC	Electronic Mode Stir Chamber (reverberation chamber)
HPM	High Power Microwave
IPT	Integrated Product Team
IR	Infrared
JON	Job Order Number
NB	Narrow Band
RF	Radio Frequency
SBIR	Small Business Innovative Research
Ti	Titanium
TWT	Travelling Wave Tube (amplifier)
WSi₂	Tungsten Di-silicide
WSiB	Tungsten Silicon Boron
ZnS	Zinc Sulfide

DEFINITIONS

<u>Word/Phrase</u>	<u>Definition</u>
Ω/square (or Ω/\square)	This is the unit for sheet resistivity. It is ohms per sheet (square) of material, but the “square” is a unitless quantity. This unit is used in the materials industry to describe the resistivity of a sheet of material based on a specific measurement method. This number multiplied by the thickness of the material results in the resistivity of the material in ohms-centimeters.
Window 3	This is the WSi_2 thin film sputtered onto a ZnS substrate with a Ti adhesive that was measured in 1994.
Window 4	This is the un-annealed WSi_2 thin film sputtered onto a AlN substrate with a Ti adhesive that was measured in this experiment.
Window 5	This is the annealed WSi_2 thin film sputtered onto an AlN substrate with a Ti adhesive. (This was Window 4 before it was annealed.)
Window 6	This is the un-annealed WSiB thin film sputtered onto a quartz substrate.
BLWGN	Band-Limited White-Gaussian Noise (BLWGN) can be used to create uniform fields in any cavity such as an aircraft fuselage or a reverberation chamber. BLWGN can be injected into an aircraft cavity to measure the shielding effectiveness of the aircraft as well as the response of electronic equipment in the aircraft.
EMSC	The Electronic Mode Stir Chamber (EMSC) method injects BLWGN into a reverberation chamber to attain a uniform electric field for the purpose of conducting electromagnetic susceptibility tests or shielding effectiveness tests.
Uniform Field	For the purpose of this report, a uniform field is defined as an isotropic, randomly polarized, equal electric field magnitude environment.

Baseline	This measurement is the shielding effectiveness of the open aperture. This establishes the minimum shielding effectiveness possible with the experiment configuration.
Dynamic Range	This measurement is the shielding effectiveness of a solid metal plate over the aperture. This establishes the maximum shielding effectiveness possible with the experiment configuration.
Shielding Data	This measurement is the shielding effectiveness with the sample over the aperture.

1.0 Introduction

1.1 Historical Background of this Small Business Innovative Research

The Air Force Research Laboratory's Directed Energy Directorate (AFRL/DE) initiated an SBIR effort in 1994. The goal of this SBIR was to determine methods to harden Infra-Red (IR) systems against Electromagnetic Interference (EMI) [1]. The windows of the IR system provide an entry path for Radio Frequency (RF) energy. Metal mesh coatings on external structures or surface-doped semiconductors are two types of conventional approaches that shield IR systems against EMI. Metal mesh coatings suffer from weather damage because the metals are mechanically soft and are affected by thermal shock. Thermal shock occurs because the metal and substrate have very different coefficients of thermal expansion. Semiconductors suffer from optical absorption problems and shielding effectiveness problems at lower temperatures.

Sienna Technologies, Inc., successfully demonstrated a third method in Phase I of its SBIR program that eliminated the problems associated with the traditional approaches. Sienna fabricated electrically conductive metal silicide (thin film) coatings that optimized IR transmission around 1 μm and between 8-12 μm , and they also maximized shielding effectiveness between 400 MHz and 18 GHz. Metal silicide coatings have similar coefficients of thermal expansion to the substrate, so there is minimal thermal shock. The silicides are highly conductive at operating temperatures and effectively shield against EMI. These silicide coatings are also hard, and they will protect against sand and rain erosion. The metal silicides are also being developed to maximize IR transmission through 1.06 μm and 1.54 μm . Sienna is conducting the research and fabricating the windows, and AFRL/DEPE is conducting RF shielding effectiveness measurements and IR transmission measurements to verify that the thin film window meets the SBIR objectives.

Phase I of this effort produced three different windows. The tungsten di-silicide (WSi_2) was delaminating, so titanium (Ti) was used to help the WSi_2 adhere better to the

substrate. This window with Ti (Window 3) had a very good RF shielding effectiveness. Experiments demonstrated a 30 dB shielding effectiveness [1]. This improvement over the shielding effectiveness of the first two windows may have been because the Ti combined chemically with the WSi_2 when the window was annealed. The resistivity of Window 3 was measured to be $0.2 \text{ } \Omega/\text{square}$ or $3.1 \text{ } \mu\Omega\text{-cm}$. This was close to the resistivity of copper ($1.7 \text{ } \mu\Omega\text{-cm}$) which is an excellent shield against RF. The thin film on Window 3 was $0.7 \text{ } \mu\text{m}$ thick, and a ZnS (zinc-sulfide) substrate was used. The IR transmission was not measured.

Sienna duplicated Window 3 and made another WSi_2 thin film with the Ti adhesive (Window 4). Sienna fabricated Window 4 to better understand the properties of the WSi_2 with Ti adhesive—including the difference between the annealed and original window. The Ti adhesive should not combine with the WSi_2 until the window is annealed, so the chemical structure of the window will be analyzed before and after annealing it to verify that the Ti combines with the WSi_2 when the window is annealed. This experiment examined the shielding effectiveness and IR transmission characteristics of Window 4. Window 4 was not annealed at the optimized temperature of $700 \text{ } ^\circ\text{C}$ in an Argon gas environment, so its resistivity was only $7.2 \text{ } \Omega/\text{square}$. (An annealed window will have a lower sheet resistivity and thus higher shielding effectiveness.) This was done to analyze the properties and structure of Window 4 before annealing it. Window 4 was $0.22 \text{ } \mu\text{m}$ thick, and an AlN (aluminum nitride) substrate was used. They measured a low conductivity of the AlN substrate, and a 20% IR transmission at $6 \text{ } \mu\text{m}$. They provided AFRL/DEPE with this substrate in order for AFRL/DEPE to measure the shielding effectiveness and IR transmission to determine if the substrate met the requirements.

Phase II of this effort is pursuing different ratios of tungsten to silicon (W_xSi_y), adding a third element to the W_xSi_y , doping silicon carbide and ceramic oxide with gold or copper to increase their conductivity, different annealing temperatures, and different types of adhesives. If the thin film windows do not provide sufficient RF shielding, then the metal mesh pattern calculated and prototyped in Phase I of the SBIR will be put over the thin film. Sienna will continue their research through the end of the SBIR in April 1999.

1.2 Purpose

The purpose of this experiment was to determine the RF shielding effectiveness of Window 4 between 400 MHz and 18 GHz and to establish the IR transmission properties of the film at 1.06 μm , 1.54 μm , and between 8 and 12 μm .

1.3 Objectives

The objectives of this experiment were to:

- Determine the shielding effectiveness of Window 4 between 400 MHz and 18 GHz. The approximate Electromagnetic Interference (EMI) shielding should be:
 - 30 dB between 400 MHz - 1 GHz
 - 25 dB between 1 - 4 GHz
 - 20 dB between 4 - 18 GHz
- Determine the IR transmission properties of the window and ensure that the window will not inhibit military IR laser systems. The transmission should be greater than 90 percent at 1.06 μm , 1.54 μm , and 8 - 12 μm .
- Verify the reverberation chamber results with anechoic chamber results. This will continue the validation of the Electronic Mode Stir Chamber technique.

1.4 Overview

Section 1 describes the background, purpose, and objectives of this experiment. The theoretical background and predictions for this experiment are in Section 2. Section 3 describes the thin film window and how the RF shielding effectiveness and IR transmission were measured. The measurement results and error analysis are in Section 4. The conclusions are in Section 5, the recommendations are in Section 6, and the list of references is in Section 7. Appendix A contains all of the graphs of data taken during the experiment.

2.0 Theoretical Background

This section predicts the shielding effectiveness of Window 4, and it explains the theory to properly conduct the shielding effectiveness measurements.

2.1 Predicted Shielding Effectiveness of Thin Film Windows

The predicted shielding effectiveness of Window 4 was 29 dB. The following is an explanation for this predicted shielding effectiveness based on the derivation by White [2].

The shielding effectiveness of a conductive material is determined by the energy it absorbs and reflects. Shielding effectiveness measurements are typically done on materials where the material is much thicker than its calculated skin depth and absorption dominates the shielding effectiveness measurement. However, electrically conductive windows are thinner than their calculated skin depth, so reflection dominates the shielding effectiveness measurement.

The shielding effectiveness of a thin film can be predicted from the measured resistivity of the thin film. Table 1 shows that the thickness (t) of Window 3 and 4 are much less than their skin depths (δ) within the specified frequency range (i.e. $t/\delta \ll 1$ for 400 MHz to 18 GHz). Measurements were made of the Windows 3 and 4 sheet resistivity (R) and of the copper conductivity (σ). The equations following Table 1 were used to populate the columns in Table 1 based on the sheet resistivity of Windows 3 and 4 and the conductivity of copper.

Table 1: Calculated Skin Depths for Different Windows

	R [$\Omega/\text{sq.}$]*	ρ [$\mu\Omega\text{-cm}$]	σ [MS/m]	$\delta_{400 \text{ MHz}}$ [μm]	$\delta_{18 \text{ GHz}}$ [μm]	$t/\delta_{400 \text{ MHz}}$ μm	$t/\delta_{18 \text{ GHz}}$ μm
Copper	0.11	1.7	58.1	3.30	0.49	0.066	0.449
Window 3	0.20	3.1	32.1	4.43	0.66	0.049	0.333
Window 4	9.20	143.1	0.7	30.06	4.48	0.007	0.049

* See the Definitions section for a description of the sheet resistivity, R .

Note that Window 3 was 0.07 m in diameter and 0.7 μm thick (t), while Window 4 was 0.1 m in diameter and 0.22 μm thick [1]. A 0.22 μm thickness was used for the

shielding effectiveness due to absorption calculations in order to directly compare the three materials. The shielding effectiveness due to reflection is only dependent on the sheet resistivity, so the reflection for a 0.7 μm thick window will be the same as the reflection for a 0.22 μm thick window.

The variable R is the sheet resistivity, ρ is the resistivity, σ is the conductivity, δ is the skin depth, and t is the thickness of the thin film. The skin depth must be calculated using the measured sheet resistivity. The skin depth is defined as

$$\delta = \frac{1}{\sqrt{\pi f \mu_m \sigma}} \quad (1)$$

where f is the frequency in hertz, and μ_m is the permeability of free space [3]. Equation 1 can be expressed in terms of the sheet resistivity by

$$\delta = \sqrt{\frac{Rt}{\sqrt{2}\pi f \mu_m}} \quad (2)$$

since the conductivity can be defined in terms of the sheet resistivity. The sheet resistivity is given by

$$R_{\text{square}} = \frac{\sqrt{2}}{\sigma t} = \frac{\rho \sqrt{2}}{t} \quad (3)$$

Table 2 shows the calculated shielding effectiveness due to absorption and reflection. The overall shielding effectiveness is

$$SE_{\text{total}} = \text{Re} \left[20 \cdot \log \left(e^{t/\delta} \cdot \frac{Z}{4} \cdot (1 - e^{-2t/\delta} e^{-j2t/\delta}) \right) \right] \quad (4)$$

where Z is defined as the ratio of the impedance of free space (open) to the impedance of the thin film, given by

$$Z = \frac{Z_o}{Z_f} = \frac{\eta_0}{\frac{\sqrt{2}}{\sigma t}} = \frac{\eta_0 \sigma t}{\sqrt{2}} \quad (5)$$

where η_0 is the free space wave impedance for a plane wave (377 Ω) [2]. Z_o is the impedance at a point without the window blocking the RF, and Z_f is the impedance at a

point with the window blocking the RF. A plane wave reflects from a material when there is an impedance mismatch ($Z \gg 1$) between the plane wave (Z_o) and the material (Z_f). This impedance mismatch is the result of a low sheet resistivity ($\approx 10 \Omega/\text{square}$). Z is much greater than one for thin films since the sheet resistivity is low. Equation 4 is a simplified version of the shielding effectiveness of a material when $Z \gg 1$. The first exponential in Equation 4 is the shielding effectiveness due to absorption, and everything else is the shielding effectiveness due to reflection. If the shielding material is thin (i.e. $t/\delta \ll 1$) then the absorption loss (the first exponential) becomes negligible, and Equation 4 can be simplified to

$$SE_{\text{reflection}} = 20 \log \left(\frac{\sqrt{2} \eta_0}{2 R} \right). \quad (6)$$

If the shielding material is thick (i.e. $t/\delta \gg 1$) then the reflection loss (the last part of Equation 4) becomes insignificant, and Equation 4 can be further simplified to

$$SE_{\text{absorption}} = 20 \cdot \log \left[e^{t/\delta} \right]. \quad (7)$$

Note that the shielding effectiveness is approximately 10 dB when the thickness, t , equals the skin depth. A good rule of thumb is a shielding effectiveness of 10 dB for every skin depth of material thickness.

Figure 1 and Figure 2 show the effects of material thickness and frequency on the shielding effectiveness. The shielding effectiveness versus frequency for a thin film (Window 4 -- $0.22 \mu\text{m}$) and a thick film (5 mm) using Equation 4 is shown in Figure 1. This figure shows that the shielding effectiveness improves with frequency only if the film is thick enough for absorption to be a significant portion of the shielding effectiveness.

The shielding effectiveness versus film thickness is shown in Figure 2 for the sheet resistivity of Window 4. This figure shows that absorption will not improve the shielding effectiveness of Window 4 in microwave frequencies until it is five millimeters thick. Thus the shielding effectiveness of Window 4 is due to reflection, and Equation 6 should be used to predict the shielding effectiveness of the thin film window. Figure 2

also shows that the shielding effectiveness for a thin film window should be constant from 400 MHz to 18 GHz.

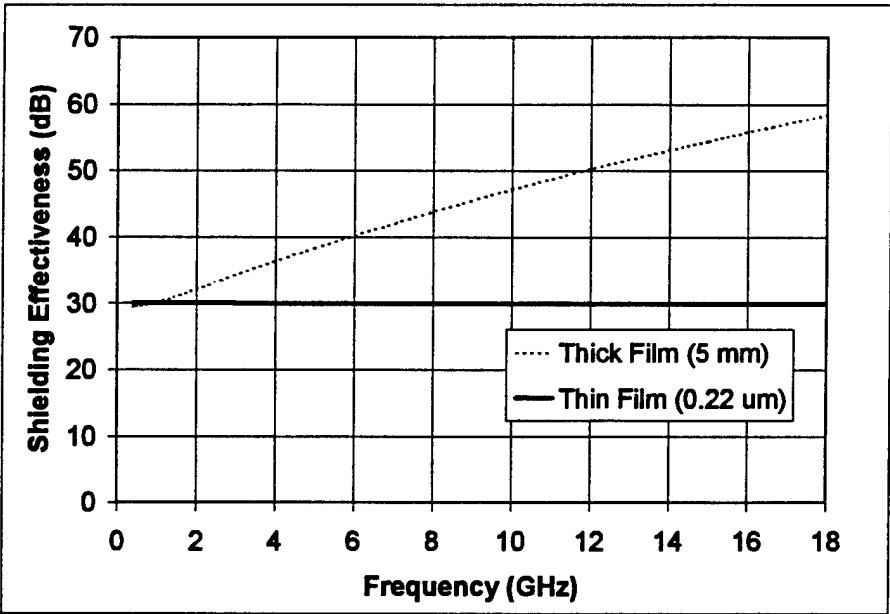


Figure 1. Predicted Shielding Effectiveness vs. Frequency for a Thin and Thick Film

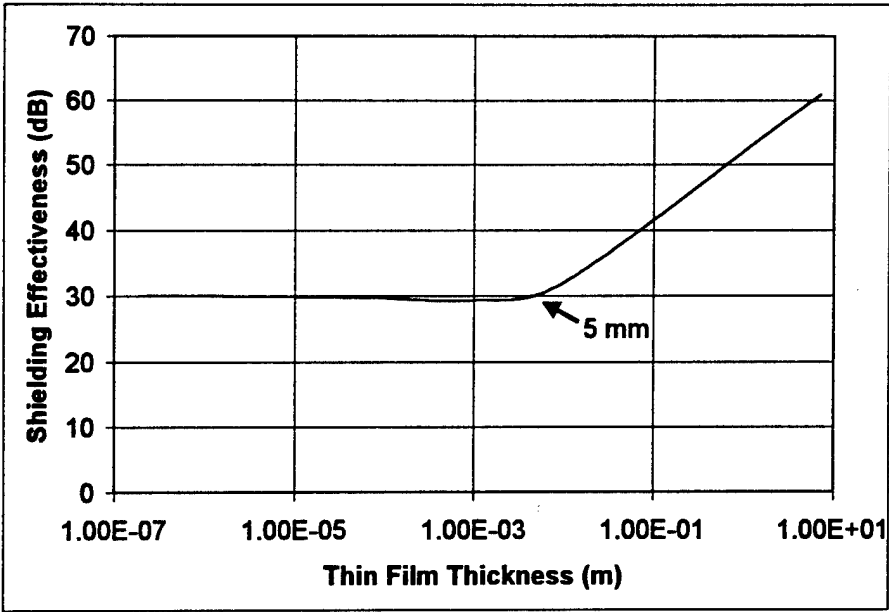


Figure 2. Predicted Shielding Effectiveness vs. Thickness for 9.2 Ω/square

Table 2 shows the predicted shielding effectiveness due to absorption and reflection for copper, Window 3, and Window 4. These predictions were based on the

previous equations, and they further show that the shielding effectiveness of Window 4 is due to reflection and not absorption.

Table 2: Predicted Shielding Effectiveness Due to Absorption and Reflection

	Absorption		Reflection	
	400 MHz [dB]	18 GHz [dB]	400 MHz [dB]	18 GHz [dB]
Copper	0.58	3.90	68	68
Window 3	0.43	2.89	59	59
Window 4	0.06	0.42	29	29

As a comparison, the shielding effectiveness due to reflection is 20 dB from 400 MHz to 18 GHz for conductive paints with a resistivity of $10 \Omega/\text{square}$ [2]. This compares well with the prediction of 29 dB for Window 4, since a $9 \Omega/\text{square}$ resistivity should result in a slightly higher shielding effectiveness.

The experimental results for the shielding effectiveness are described in Section 4.1. The following sections develop the theory to properly perform the shielding effectiveness measurements.

2.2 Isolation between the Reverberation Chamber and the Nested Chamber

Precautions must be taken so that the reverberation chamber does not affect the measurements in the nested chamber. A measurement in the nested chamber must be isolated from a measurement in reverberation chamber when there is no thin film window in the aperture of the nested chamber. (See a diagram of the experimental setup in Figure 3 of the next section.) Improper isolation will cause the measurement method to affect the measured values. Proper isolation occurs when the power density inside the nested chamber is at least 10 dB lower than the power density in the reverberation chamber over the frequency range of interest [4]. Isolation is important to ensure accuracy and repeatability in the measurement.

The circular aperture of the nested chamber will attenuate RF, and thus isolate fields inside the nested chamber from fields in the reverberation chamber. The shielding effectiveness for an aperture is

$$SE_{reflection} = 99 - 20\log(d \cdot f_{MHz}) \quad (8)$$

where d is the diameter of the aperture in millimeters and f_{MHz} is the frequency in megahertz [2]. The predicted shielding effectiveness for a 4" diameter at 400 MHz is 7 dB, and the shielding effectiveness above 800 MHz is 0 dB. Equation 8 can only be used when the frequency is less than $c/2d$.

Another method to predict the shielding effectiveness of an aperture is through an analysis of the cutoff frequency of the aperture. In general, the cutoff frequency is

$$f_c = \frac{1.841 c}{\pi d} \quad (9)$$

where f_c is the cutoff frequency of the TE_{11} mode in a circular waveguide, d is the diameter of the aperture, and c is the speed of light [3]. The cutoff frequency for the 0.1-m diameter aperture thin film window is 1.7 GHz. The cutoff frequency implies that all RF will pass through this aperture above 1.7 GHz. This agrees with the result from Equation 8 that all RF above 800 MHz will pass through this aperture (i.e. have a shielding effectiveness of 0 dB).

The shielding effectiveness of the nested chamber aperture can be approximated from shielding effectiveness measurements of apertures of similar diameter. The 0.1 m diameter of the nested chamber is similar to the diameter (0.07 m) of an aperture tested by Loughry [4]. This aperture has a shielding effectiveness of around 10 dB between 4.0 and 8.0 GHz. Equation 8 and Equation 9 predict no shielding at these frequencies, so some other type of interaction must be occurring to result in a greater aperture shielding effectiveness. Using the previous measurements as a prediction, the 0.1 m diameter should provide sufficient isolation since its diameter is similar to the small aperture tested by Loughry. The experimental results are shown in Section 4.3.

2.3 Lower Operating Frequency of the Nested Chamber

The lower operating frequency can be determined from the number of independent modes in a reverberation chamber. The theoretical number of independent modes is defined by

$$\Delta N = \frac{8\pi V}{c^3} f^2 \cdot NBW \quad (10)$$

where ΔN is the number of independent modes, V is the volume of the chamber, c is the speed of light, f is the frequency, and NBW is the noise bandwidth [5]. Equation 10 can be rearranged to determine the lowest operating frequency

$$f = \sqrt{\frac{\Delta N c^3}{8\pi V \cdot NBW}} \quad (11)$$

The following table shows the theoretical lower operating frequency for a 50 MHz and 100 MHz noise bandwidth in the nested chamber. The following parameters were used in this equation. The nested chamber was 0.6 m wide, 0.76 m deep, and 0.6 m tall. An acceptable field uniformity in a reverberation chamber is ± 3 dB or less, and the number of independent modes (ΔN) to maintain a ± 3 dB field uniformity is 57 or more [5].

Table 3: Minimum Operating Frequency for Nested Chamber

Noise Bandwidth (MHz)	Minimum Frequency (MHz)
50	2.0
100	1.5

Table 3 shows that the minimum operating frequency for the nested chamber with a 50 MHz NBW is 2 GHz. The minimum operating frequency for a 100 MHz NBW is 1.5 GHz. This shows that the nested chamber will not provide sufficient field uniformity below 1.5 GHz. The 100 MHz noise bandwidth should not be used anyway since the noise bandwidth should be kept less than one tenth of the center frequency [4]. The experimental results are shown in Section 4.4.3.

2.4 IR Transmission

The infra-red (IR) transmission should be between 60% and 75% for $9 \Omega/\text{square}$ based on conductive glass measurements [2]. The variation results from different substrate types, metal types, and adhesion techniques. The IR transmission of the past thin film windows was not measured, but calculations show that the theoretical IR transmission for WSi_2 is 90% [6].

3.0 Experimental Setup

There were four parts to this experiment: three shielding effectiveness measurements and one infra-red (IR) transmission measurement. The first set of measurements injected BLWGN into a reverberation chamber owned by AFRL/DEPE. This measurement provided a quick overview of the average shielding effectiveness of the thin film window, and it is called the Electronic Mode Stir Chamber (EMSC) technique. The second set of measurements injected BLWGN into an anechoic chamber owned by AFRL/DEPE. These measurements provided the shielding effectiveness of the window versus angle of incidence. This measurement most closely simulated the real environment that the thin film windows will experience, because, in reality, the thin film window will be mounted on an aperture into the cavity. Electromagnetic waves will enter from a free field environment (simulated by the anechoic chamber) and enter into the cavity (simulated by a reverberation chamber). The third set of measurements was the Continuous Wave (CW) measurement. This measurement used the same anechoic chamber as the BLWGN measurements, and it was intended to validate the BLWGN measurements. Proper measurements could not be made with this setup as described in Section 4.0. The fourth set of measurements was the IR transmission measurements done using a spectrophotometer at a laser research facility owned by AFRL/DEPE.

3.1 Materials Tested

In all three shielding effectiveness measurements, one window and two substrates were tested. The thin film was sputtered onto a polished Aluminum Nitride (AlN) substrate and Titanium (Ti) was used to help the thin film adhere to the AlN (Window 4). A polished AlN substrate and unpolished AlN substrate were also tested. These were not labeled as a "windows" since they do not have any thin film material sputtered onto them. They will be referred to as the "polished" and "unpolished" substrates. The thin film material is always sputtered onto a polished substrate to maximize IR transitivity, so any reference to a substrate is assumed to be a polished substrate. The audience at EMC Roma '96 questioned the shielding effectiveness that the substrate contributed to the window, so this experiment also measured the shielding effectiveness of the polished substrate without the thin film. This demonstrated the shielding effectiveness of the

substrate alone, so the actual shielding effectiveness of the thin film could be extracted. The substrate should not and did not contribute to the overall shielding effectiveness of the window. The unpolished substrate was measured to determine if there is a difference in shielding effectiveness between the polished and unpolished substrate--no difference was expected.

The window and substrates were 0.1 m in diameter and about 1 mm in thickness. Window 4 and the substrates all had a gold contact pad on the outer edge to enhance the electrical conductivity with the nested chamber. The nested chamber was 0.6 m wide, 0.76 deep, 0.6 m tall, and made of 0.3 cm thick aluminum.

3.2 Reverberation Chamber Experimental Setup

The following were the procedures for conducting experiments in the reverberation chamber using the Electronic Mode Stir Chamber (EMSC) method. For a more basic description of the EMSC technique, see [5].

Figure 3 shows the general setup used for the measurements in the reverberation chamber. The thick lines indicate General-Purpose Interface Bus (GPIB) lines and the thin lines indicate RF cables.

The data acquisition system on the computer controlled all of the instruments via the GPIB. The HP 8757C Scalar Network Analyzer controlled the HP 83620 Synthesized Sweeper. The computer routed the signal to the correct amplifiers and mixers. The signal originated from the sweeper and then was up-converted and mixed with the NC 7907 White-Gaussian Noise Source. Twenty-Watt Traveling Wave Tubes (TWT) amplified the Band-Limited White-Gaussian Noise (BLWGN) and then transmitted it into the reverberation chamber through a broadband horn antenna. The EMSC method is defined as radiating BLWGN into a reverberation chamber. Three B-Dot probes measured the fields inside the nested chamber, and one B-Dot probe measured the fields inside the reverberation chamber.

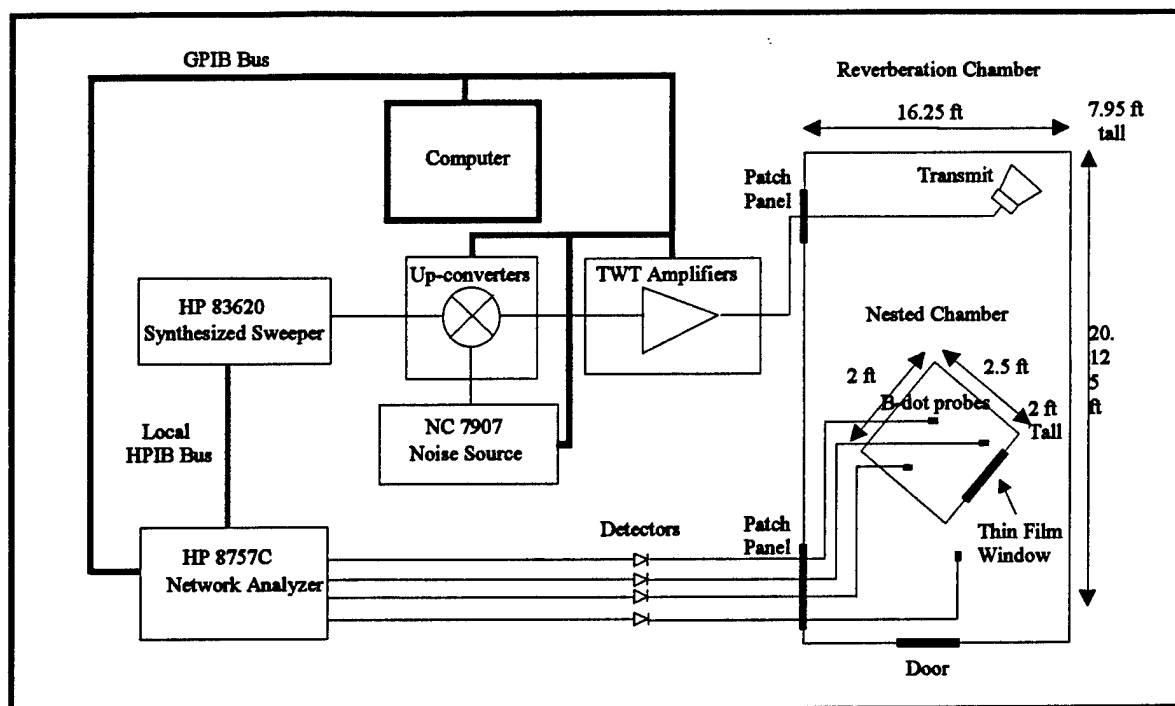


Figure 3: EMSC Experimental Setup

The B-Dot probes measured the changing magnetic field, and the detectors converted this field level into a DC signal for the HP 8757C Network Analyzer to measure. Data was collected over the GPIB bus by the data acquisition system on the computer. Steel wool was used over the cables connecting to the feed-through panel of the nested chamber preventing RF from coupling through the cables instead of the thin film window. The nested chamber was positioned at an angle to the wall of the large chamber in order to facilitate the excitation of more modes.

3.3 Band-Limited White-Gaussian Noise Experimental Setup

Band-Limited White-Gaussian Noise (BLWGN) was radiated onto the metal box in the anechoic chamber. The BLWGN induced uniform fields in the small chamber, so the power transmitted through the window could be measured. Multiple incident angles were used to measure the shielding effectiveness versus incident angle.

Field uniformity measurements were done again in the nested chamber using the method described above. Fields were radiated at normal incidence to the thin film window to achieve maximum transmission through the film. The setup for the shielding effectiveness measurements is shown in Figure 4.

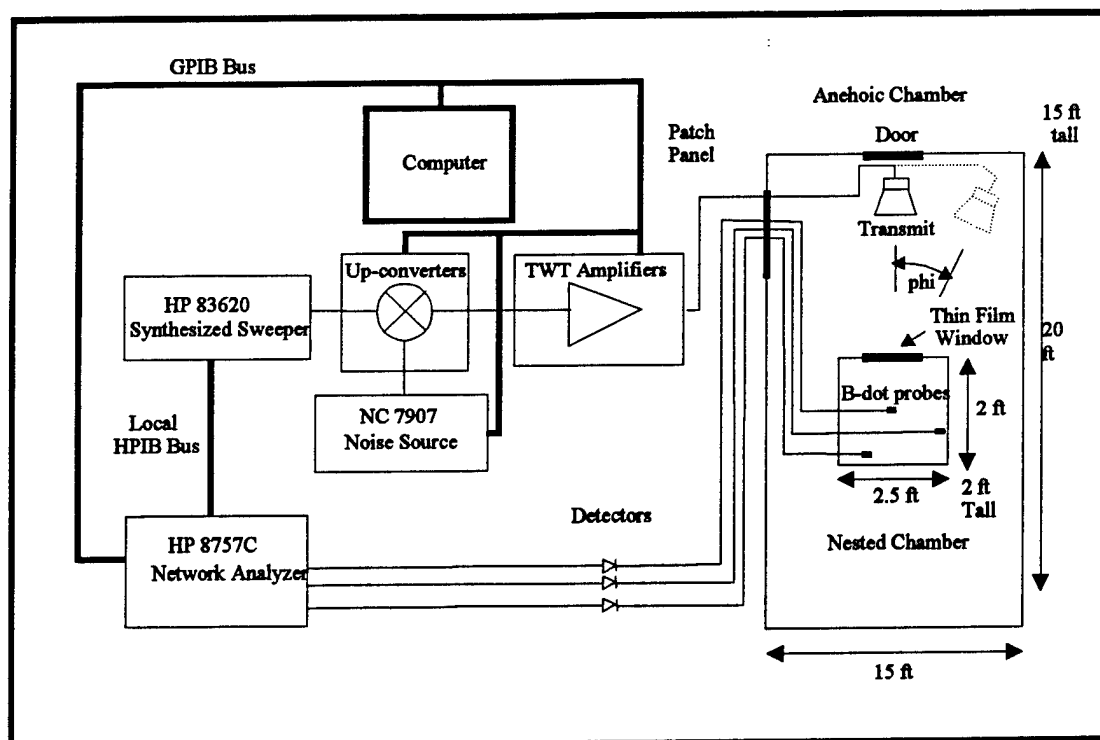


Figure 4: BLWGN Experimental Setup

Figure 4 shows that the transmitting antenna was moved ϕ (ϕ) degrees to measure the shielding effectiveness versus incident angle, and the nested chamber was setup at the far side of the chamber from the door. BLWGN was created and radiated into the chamber in the same way it was in the reverberation chamber. In this case, the walls absorbed the RF instead of reflecting it. Three probes were inside of the nested chamber to measure the field uniformity and the RF received through the window.

3.4 Continuous Wave Anechoic Chamber Experimental Setup

This section describes the CW measurements. These measurements were intended to examine the shielding effectiveness of the window in an anechoic environment. This is a more traditional method to perform shielding effectiveness measurements, and the results were intended to validate the EMSC and BLWGN approaches.

Figure 5 shows the setup used for these measurements.

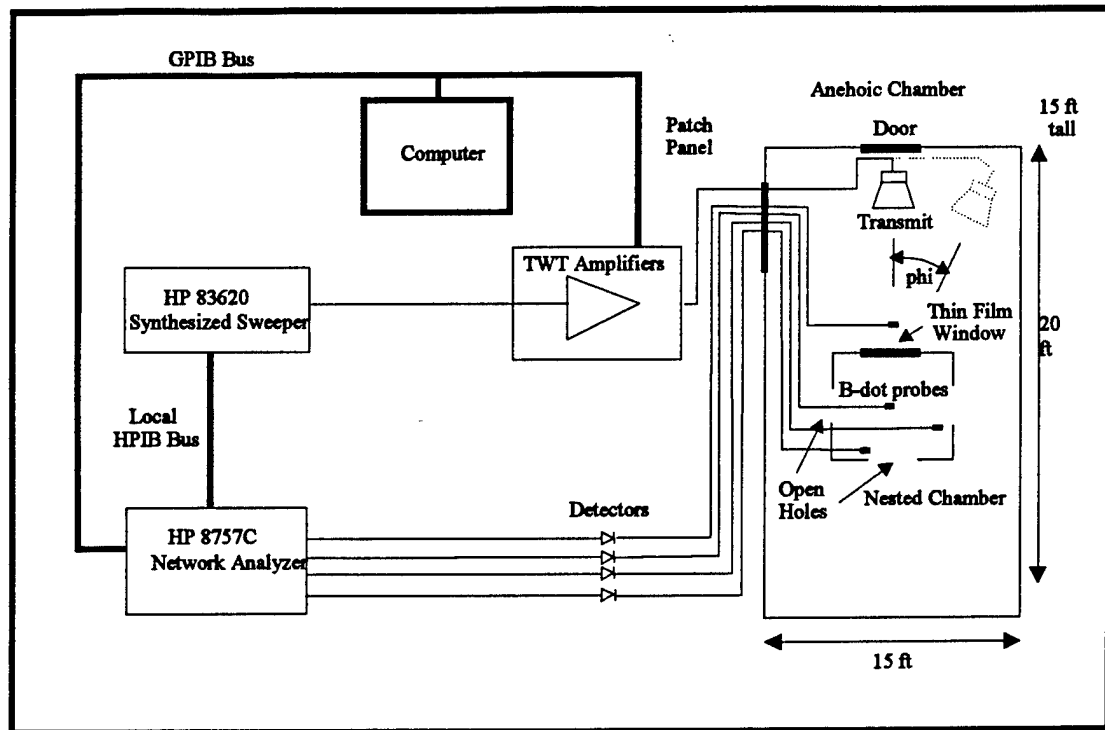


Figure 5: CW Experimental Setup

All of the apertures in the nested chamber were left open and anechoic material was put inside it to keep it from acting like a reverberation chamber. Section 4.0 will explain why these measures were not enough to keep it from acting like a reverberation chamber. The metal around the aperture with the samples kept source RF from coupling to the probe in the box.

Figure 5 shows that the transmitting antenna was moved ϕ (ϕ) degrees to measure the shielding effectiveness. The box was setup at the far side of the chamber from the door, and three probes were inside of the nested chamber to determine if it was acting like a reverberation chamber. The same data acquisition software was used for the CW, ESMC, and BLWGN measurements.

3.5 Antennas Used

The same antennas were used in the reverberation and anechoic chambers. A dual-ridged wideband horn antenna was used to transmit RF into the chamber. This antenna was rated from 1 to 18 GHz. B-dot probes were used inside of the nested

chamber to measure the RF that penetrated through the window. B-dot probes were chosen because three probes in the chamber would not load the chamber (i.e. adversely affect the measurement.) These probes were rated from 1 to 12 GHz. The B-dot probes were not sensitive enough below 1 GHz (i.e. their diameter was less than one tenth the wavelength), and the RF was not uniform across the probe above 12 GHz (i.e. their diameter was greater than the wavelength). One set of antennas was used to quickly evaluation the thin film window without having to used multiple antenna configurations. The loss in effectiveness of these antennas was taken into account when they were used out of their range.

3.6 Laser Measurements

The laser effects research facility in AFRL/DEPE performed the IR transmission measurements. Established procedures for IR transitivity measurements were followed. A spectrophotometer from 1 to 2.5 μm and 2.5 to 50 μm was used.

4.0 Measurement Results

This section contains the results from the experiment. See a complete listing of the graphs at the end of this document.

4.1 Shielding Effectiveness Measurements

This section describes how the shielding effectiveness measurements were taken, and it shows the shielding effectiveness data for the EMSC measurements and the BLWGN measurements.

4.1.1 Shielding Effectiveness Data Collection

The shielding effectiveness is the power density with the material in the aperture subtracted from the power density with an open aperture, since the aperture provides sufficient isolation between the large reverberation chamber and the nested chamber for the EMSC measurements [2]. (See Section 4.3.)

$$SE = \frac{S_{open}}{S_{film}} \quad (12)$$

where S is the power density. Equation 12 can be simplified to be the ratio of power levels since the volume units cancel each other.

$$SE = \frac{P_{open}}{P_{film}} = P_{open}^{dB} - P_{film}^{dB} \quad (13)$$

This division becomes a subtraction when the power densities are converted to dB.

The procedures for taking an open aperture (baseline), thin film window (shielding data), and closed aperture (dynamic range) measurement as described by Hatfield [5]. The open aperture measurement determines the shielding effectiveness of the small chamber and its open aperture. The ratio of a probe measurement behind the open aperture to a probe measurement behind the thin film window is the shielding effectiveness of the thin film. The closed aperture measurement is done with a metal plate over the aperture of the nested chamber.

The ratio of the open aperture measurement to the closed aperture measurement is the maximum shielding effectiveness measurement possible (the dynamic range). A shielding effectiveness larger than the dynamic range cannot be measured.

4.1.2 EMSC Measurements

Figure 6 shows the shielding effectiveness of the thin film—the ratio of the thin film measurement to the open aperture measurement.

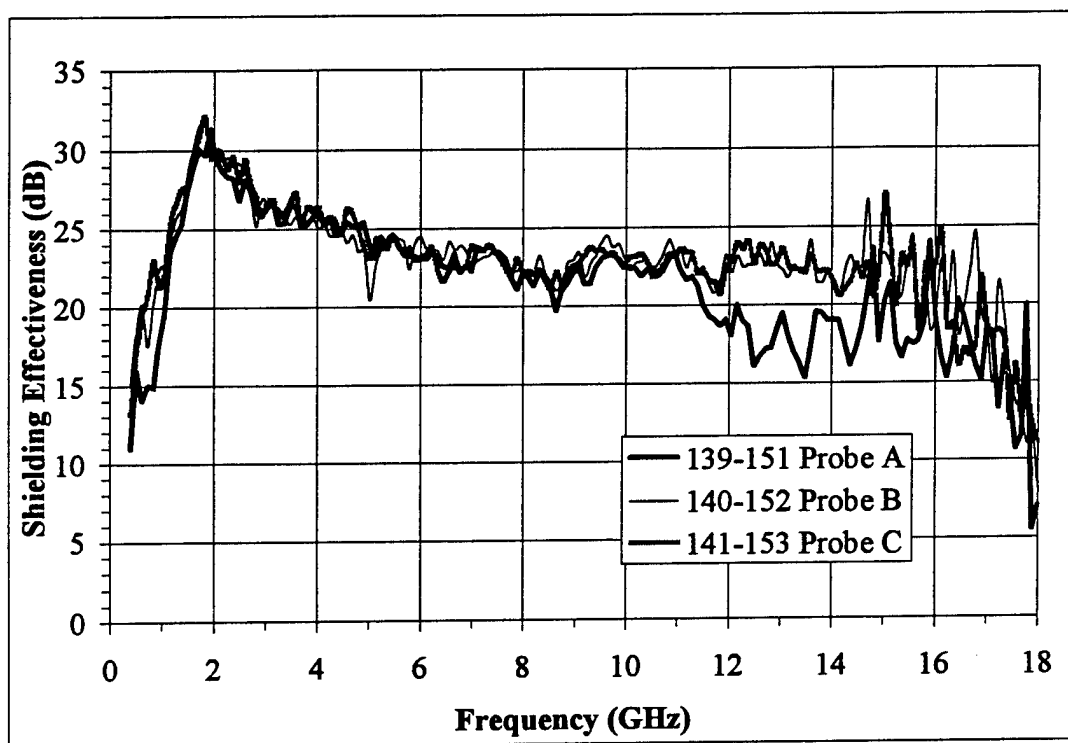


Figure 6: Shielding Effectiveness of the Thin Film Using the EMSC

Figure 6 shows that the average shielding effectiveness of every incident angle onto Sample 4 was 22 dB from 4 to 12 GHz. The measurements outside these frequencies were erratic as explained below. Figure 7 shows the shielding effectiveness of the polished substrate.

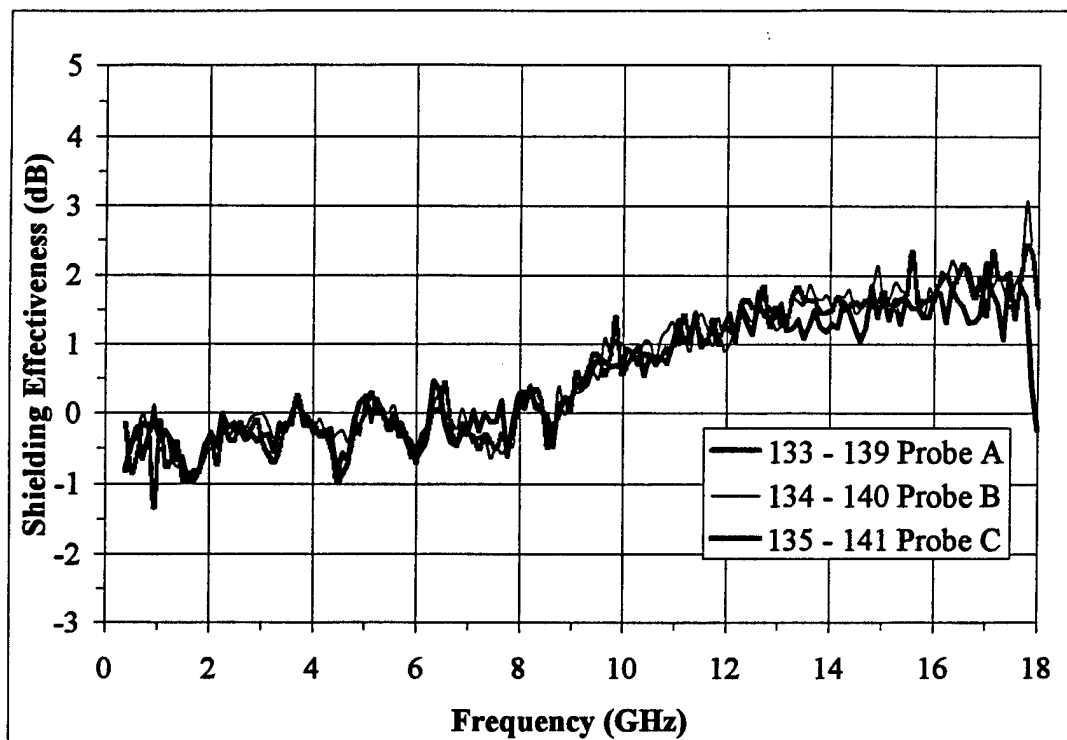


Figure 7: Shielding Effectiveness of the Polished Substrate Using the EMSC

This shows that the polished substrate did not contribute to the shielding effectiveness of the thin film. The apparent increase in shielding effectiveness with frequency was not conclusive, since the 2 dB increase was below the ± 5 dB measurement uncertainty shown in Section 4.5.

Figure 8 overlays the power measured inside the nested chamber with the aperture open, thin film over the aperture, and aperture closed. Probe C was used since one probe measurement was equal to any probe measurement in the nested chamber. It shows that the thin film measurement was in the noise floor from 400 MHz to 1 GHz, and from 14 GHz to 18 GHz. Section 4.5 shows that a lack of field uniformity in the nested chamber contributed more than 3 dB of error from 400 MHz to 4 GHz. Section 3.5 explains that the B-dot probes do not provide good measurements above 12 GHz, and so the shielding effectiveness is only known from 4 GHz to 12 GHz.

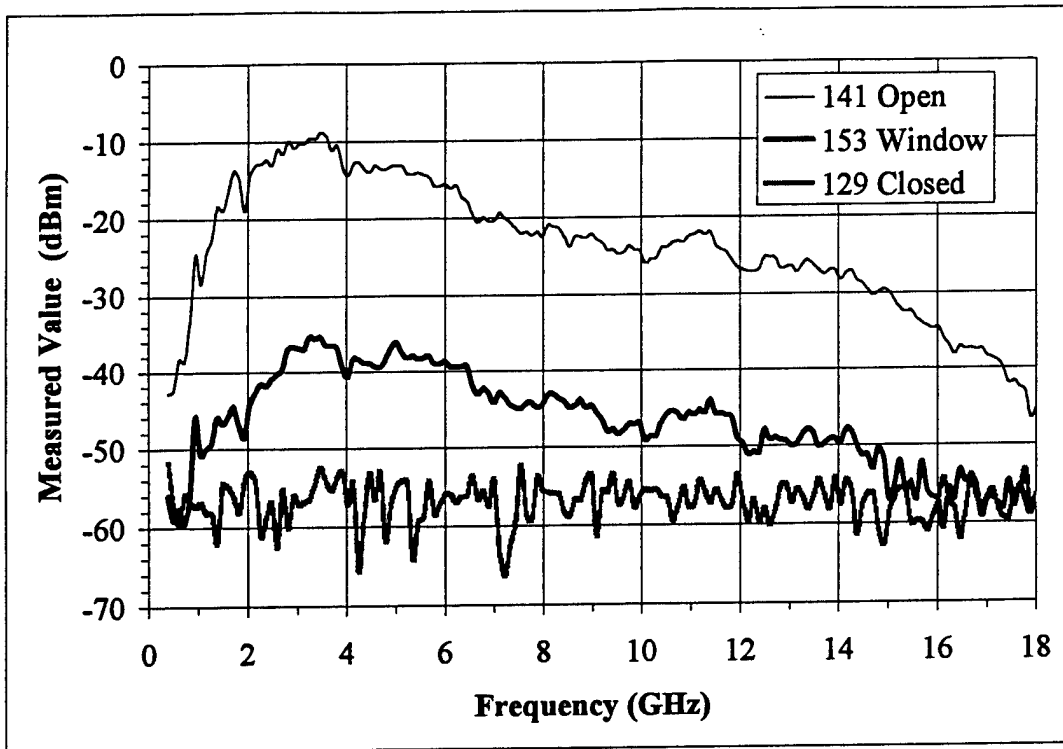


Figure 8: Overlay of the Open Aperture, Thin Film, and Closed Aperture

4.1.3 BLWGN Measurements

Figure 9 shows the shielding effectiveness of the thin film at 0.24 m from the window, zero degrees incident angle, and using a 100 MHz NBW. Probe B measured a higher value than Probe A and Probe C because it was directly illuminated by the source. Probe C was used since the transmitting antenna did not directly illuminate it, thus it only measured the field reverberating in the nested chamber. The source antenna in a reverberation chamber must never directly illuminate probes. Probes must measure the field level resulting from the superposition of waves reverberating in the chamber [5]. This is why the source antenna is always directed into a corner of the reverberation chamber.

The shielding effectiveness of the thin film versus angle of incidence could not be measured because the TWTAs did not provide enough power at a sufficient distance. The 200-Watt TWTAs will be used in the future. The only BLWGN measurements were done with the source close to the window (0.24 m), and no angle of incidence information could be taken at this distance.

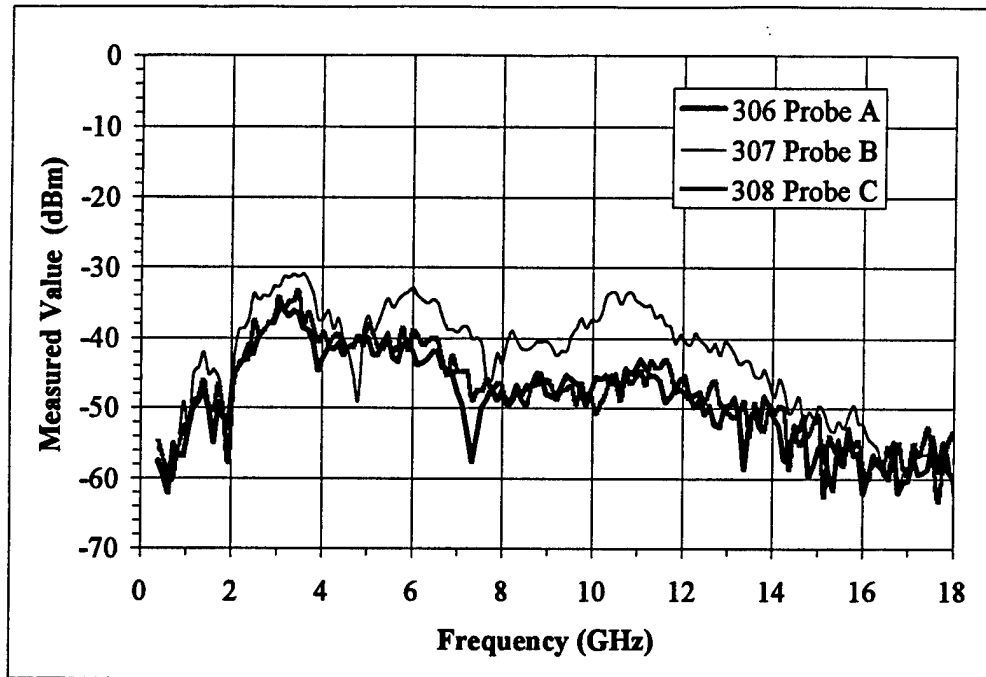


Figure 9: Shielding Effectiveness of the Thin Film at 0° Incidence Using BLWGN

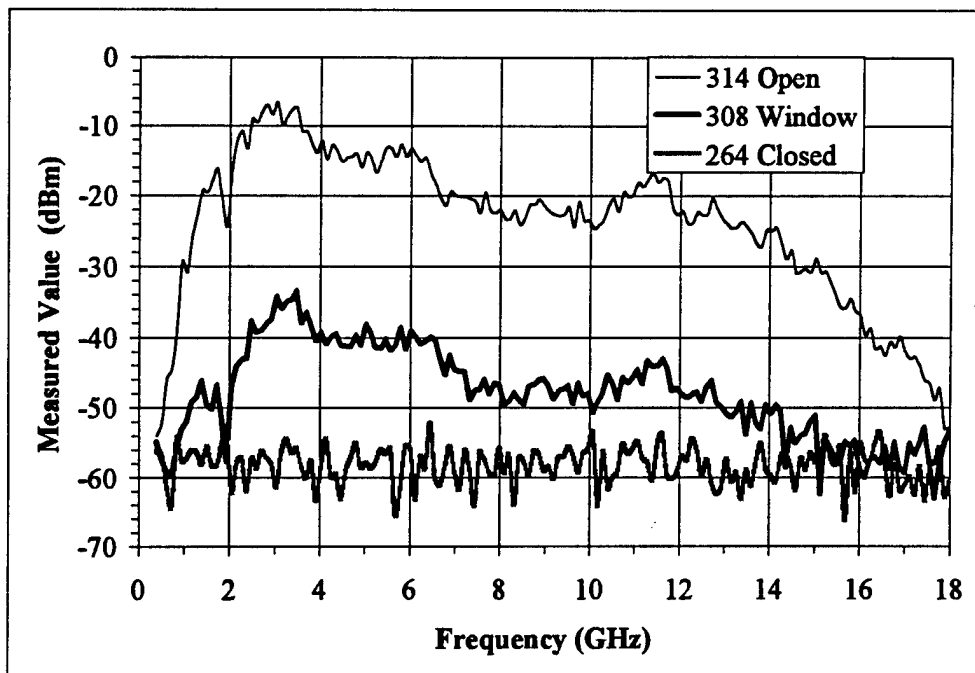


Figure 10: Overlay of the Open Aperture, Thin Film, and Closed Aperture Measurements at 0° Incidence Using BLWGN

Figure 10 overlays the open aperture, thin film over the aperture, and closed aperture measurements at normal incidence (0°) and 0.24 m from the window.

4.1.4 CW Measurements

The CW measurements were not done because it was not possible to keep the nested chamber from acting like a reverberation chamber. Plates were removed from the nested chamber and anechoic chamber material was placed inside, but these were ineffective in transforming the nested chamber into a small anechoic chamber. Figure 11 below shows the sporadic results from these attempted measurements. The 10 – 20 dB fluctuations in power indicate that areas of high intensity and low intensity radiation exist (as they exist in a non-stirred reverberation chamber), and the fields are not behaving like fields in free space. The EMSC could not be validated since the CW measurements were not possible.

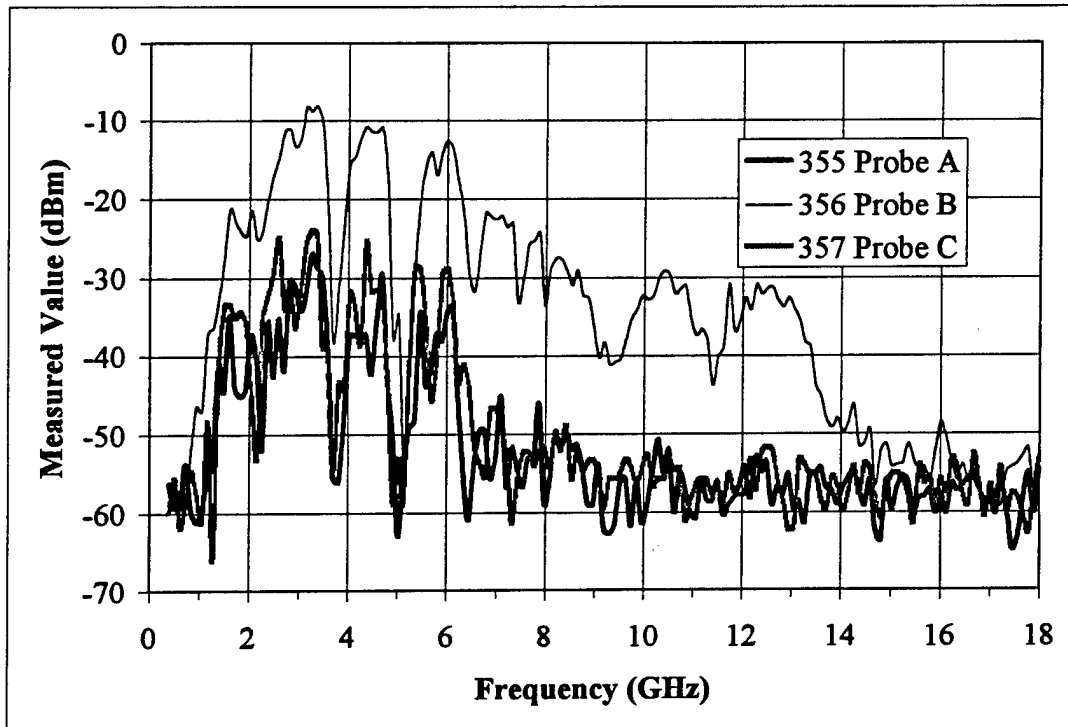


Figure 11: Attempted CW Measurement

4.1.5 BLWGN and EMSC Comparison

BLWGN and EMSC measurements are different, therefore one set of data must be corrected to compare it to the other. In an EMSC measurement, a probe in the nested chamber will measure the average of all the incident angles and polarizations. In a BLWGN measurement, a probe in the nested chamber will only measure one incident angle and polarization.

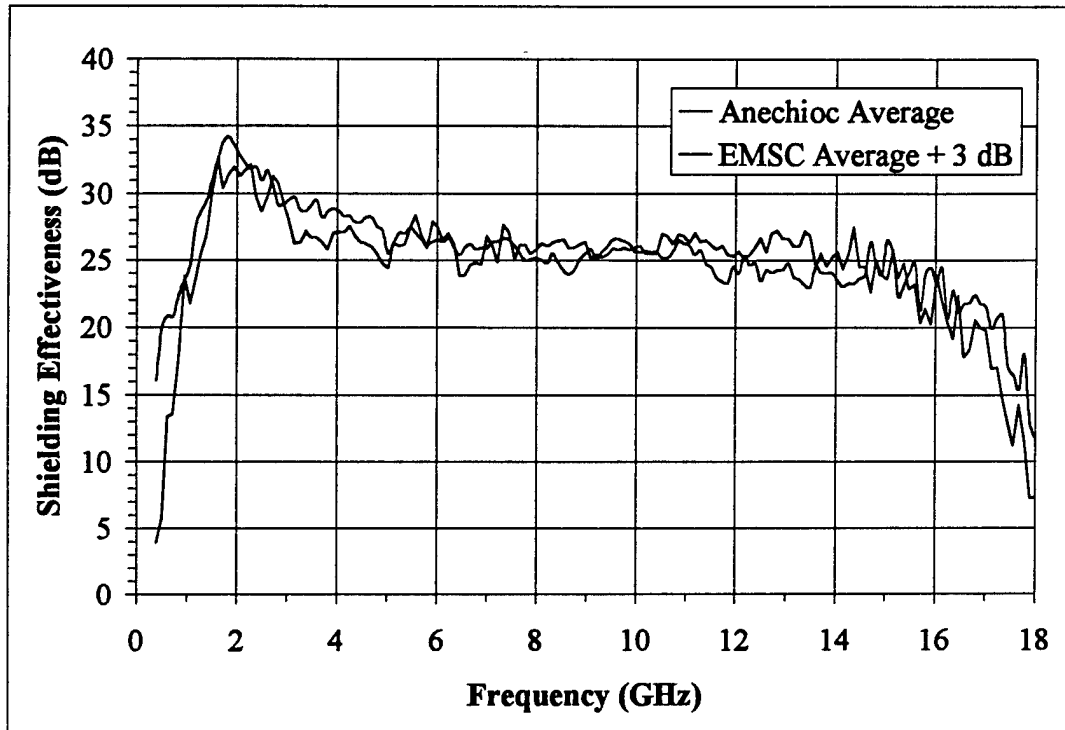


Figure 12: Comparison of the EMSC and BLWGN SE Measurements

The power into the nested chamber will decrease as the incident angle (from perpendicular) increases since aperture is circular [3]. An average of all these incident angles is approximately half of the power at normal incidence. The BLWGN measurement will be twice the power of (3 dB more than) the EMSC measurement because the EMSC is averaging all of the incident angles and polarizations at once. The EMSC data can be corrected to compare it to the BLWGN data by adding 3 dB to the EMSC measurement. Figure 12 shows the average of the three EMSC probes plus 3 dB and the average of two 0.24-meter-distant BLWGN measurements.

Figure 12 shows that the EMSC and BLWGN both measured the shielding effectiveness to be 25 dB between 4 GHz and 12 GHz. This was a good agreement between two separate experiment configurations. Angle of incidence information could not be obtained from the BLWGN measurements because the TWTAs did not provide enough power at a sufficient distance.

4.2 Measured Losses

The Travelling Wave Tube Amplifiers (TWTAs) were not powerful enough to inject enough energy for a sensor to measure the low and high frequencies. A typical graph is shown in Figure 8. Loss at the low frequency (400 MHz to 1 GHz) was due to using the transmitting horn and B-Dot probes below their minimum operating frequency (1 GHz). The B-Dot probes were used because they do not significantly load the small nested chamber, they will measure in their far-field region inside the chamber, and they are small enough to fit in the nested chamber. A larger horn antenna is appropriate for this frequency range, but it would not fit inside the nested chamber. Even if it did fit, it would lower the Q of the nested chamber and distort the measurements. A significantly larger amplifier can compensate for the loss in antenna efficiency due to operating below the antenna's operating frequency. Figure 8 shows that the TWTAs did not provide enough power to keep the probe measurement above the noise floor from 400 MHz to 1 GHz nor from 14 GHz to 18 GHz.

The loss at the high frequencies (15 GHz to 18 GHz) was due to attenuation through the mixers. Mixer loss could not be avoided. A larger amplifier can compensate for the mixer losses at the higher frequencies. Further, the high frequency measurements may be spurious, since B-dot probes do not provide good results above 12 GHz (Section 3.5).

Note that these measured losses cancelled out when the shielding effectiveness was calculated, but they did prevent shielding effectiveness measurements at the low and high frequencies since no power was measured. The lack of field uniformity in the nested chamber prevented measurements from 1 to 4 GHz. In effect, shielding effectiveness values could only be measured between 4 GHz and 12 GHz.

4.3 Isolation Measurements

The aperture on a nested chamber must provide sufficient isolation from the surrounding reverberation chamber. Figure 13 shows that the nested chamber provided sufficient (more than 10 dB) isolation between the large reverberation chamber and the nested chamber.

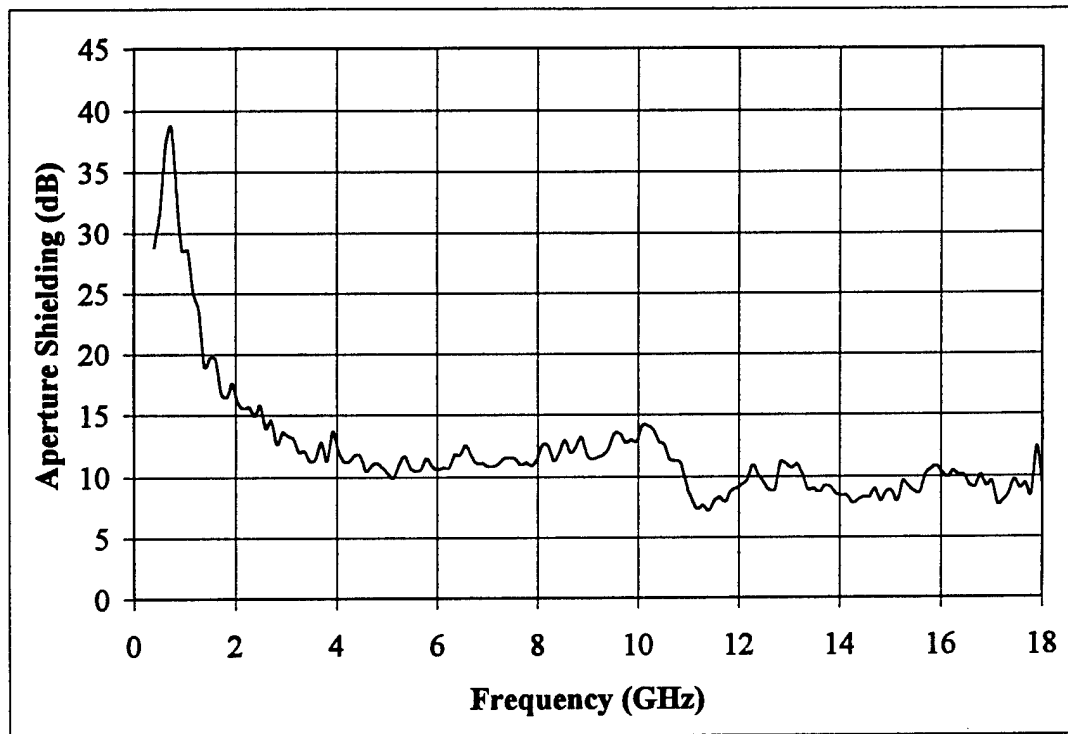


Figure 13: Isolation Provided by the Nested Chamber Aperture

The measurement shown in Figure 13 agrees with the comparison to a past measurement as described in Section 2.2. Both of these measurements show that the isolation remains constant with frequency while the calculation used to predict the isolation requires the isolation to decrease with frequency. The calculations used to predict the isolation between the reverberation chamber and nested chamber should be investigated further. The larger isolation below 3 GHz is due to the measurements approaching the noise floor, so in reality the nested chamber may not be more isolated from the reverberation chamber below 3 GHz.

4.4 Field Uniformity Measurements and Lower Operating Frequency

This section describes the field uniformity measurements done during the EMSC measurements and the BLWGN measurements.

4.4.1 EMSC Measurements

Field uniformity was measured in the large reverberation chamber, in the nested chamber while it was in the large reverberation chamber, and in the nested chamber while it was in the anechoic chamber. Sufficient field uniformity is ± 3 dB among measurements from any location and probe orientation in the chamber. A field uniformity of ± 3 dB was calculated through Monte Carlo simulations and verified through experimentation to be equivalent to two-and-a-half standard deviations [5].

Figure 14 shows the field uniformity in the large chamber using 50 and 100 MHz NBW.

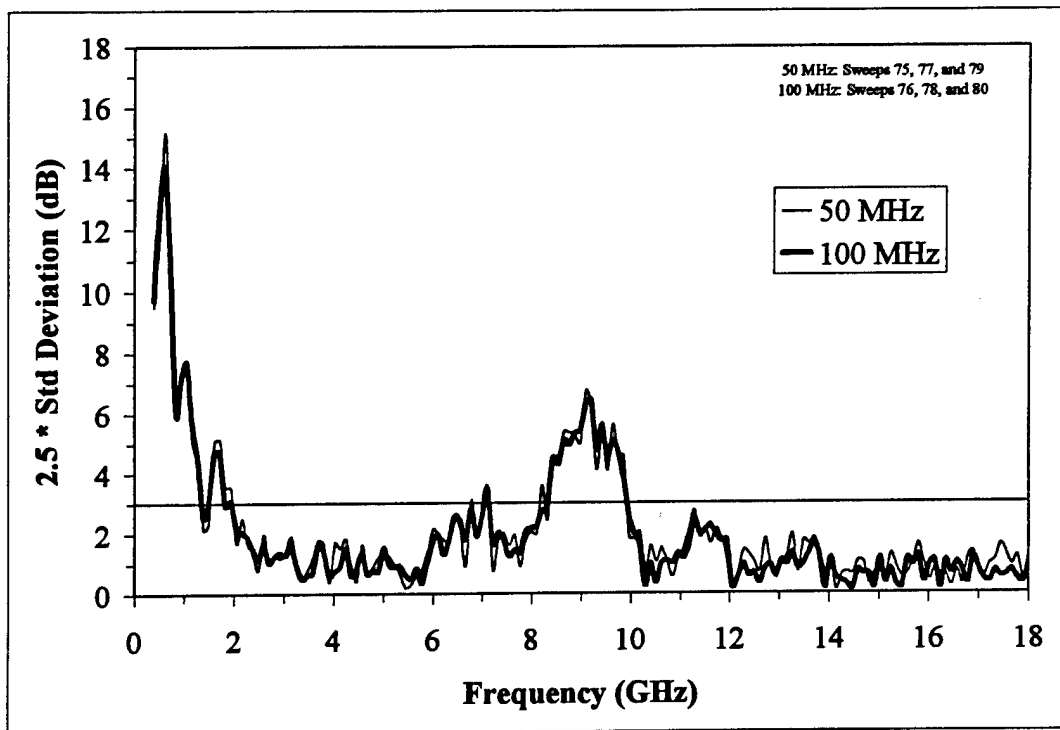


Figure 14: Field Uniformity in the Large Chamber Using a 50 and 100 MHz NBW

Figure 14 shows that the large chamber provided sufficient field uniformity from 2 GHz to 18 GHz with both the 50 MHz and 100 MHz noise bandwidths. Note that sufficient field uniformity was maintained above 12 GHz despite being out of the measurement range of the B-dot as described in Section 3.5. The lack of field uniformity around 9 GHz cannot be explained.

The noise bandwidth should be less than one-tenth of the lowest operating frequency ($10 \cdot \text{NBW} < f_{c \text{ min.}}$), but it should be as wide as possible to provide the maximum field uniformity. This implies that the 100 MHz noise bandwidth should not be used below 1 GHz, so the 50 MHz noise bandwidth was used. Calculations in Section 2.3 showed that the 50 MHz noise bandwidth would not provide sufficient field uniformity in the nested chamber below 2 GHz. The field uniformity was the same for the 50 MHz and 100 MHz NBW in the large chamber.

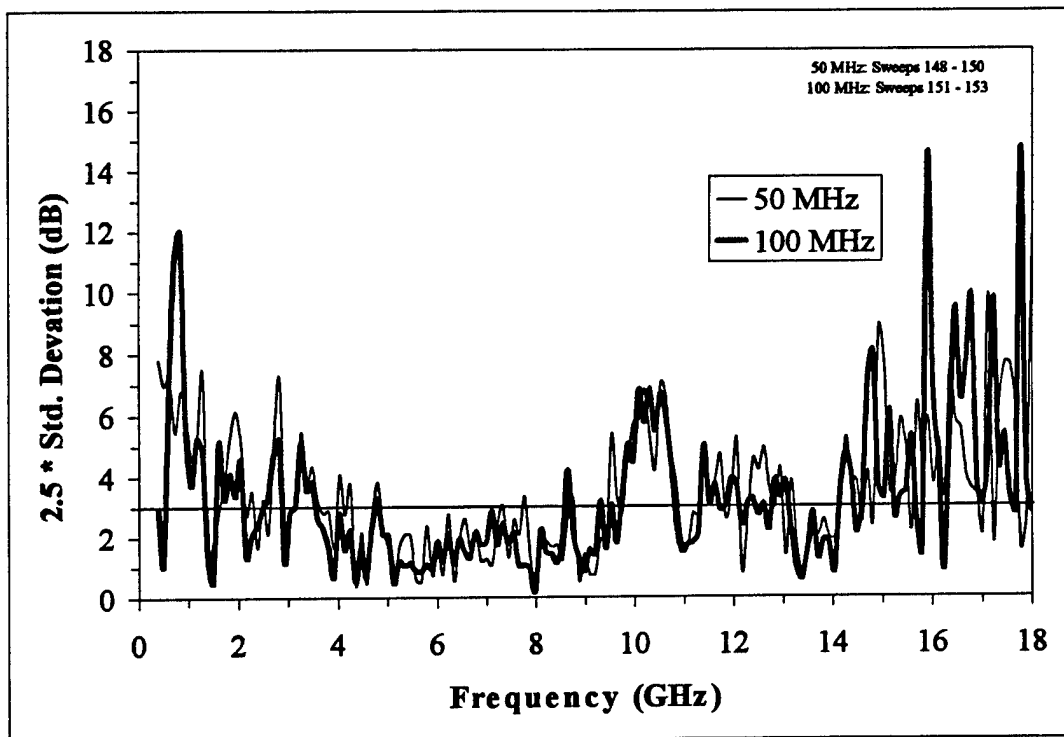


Figure 15: Field Uniformity in the Nested Chamber Using a 50 and 100 MHz NBW

The 100 MHz NBW was chosen because theoretically it could provide sufficient field uniformity down to 1.5 GHz. A 100 MHz noise bandwidth was used despite

its averaging of field variations around the center frequency since $f_{c\min} < 10 \cdot \text{NBW}$. The shielding effectiveness was expected to be fairly flat, so this large average around the center frequency did not adversely affect the measurements.

The field uniformity in the nested chamber was sufficient (i.e. less than 3 dB) for 4 GHz to 14 GHz for every test sample mounted it. Sufficient field uniformity was measured in the Nested Chamber and large chamber using the EMSC technique. It is not understood why there was a lack of field uniformity around 10 GHz in the nested chamber.

4.4.2 BLWGN Measurements

Figure 16 shows the field uniformity between two probes during the BLWGN experiment.

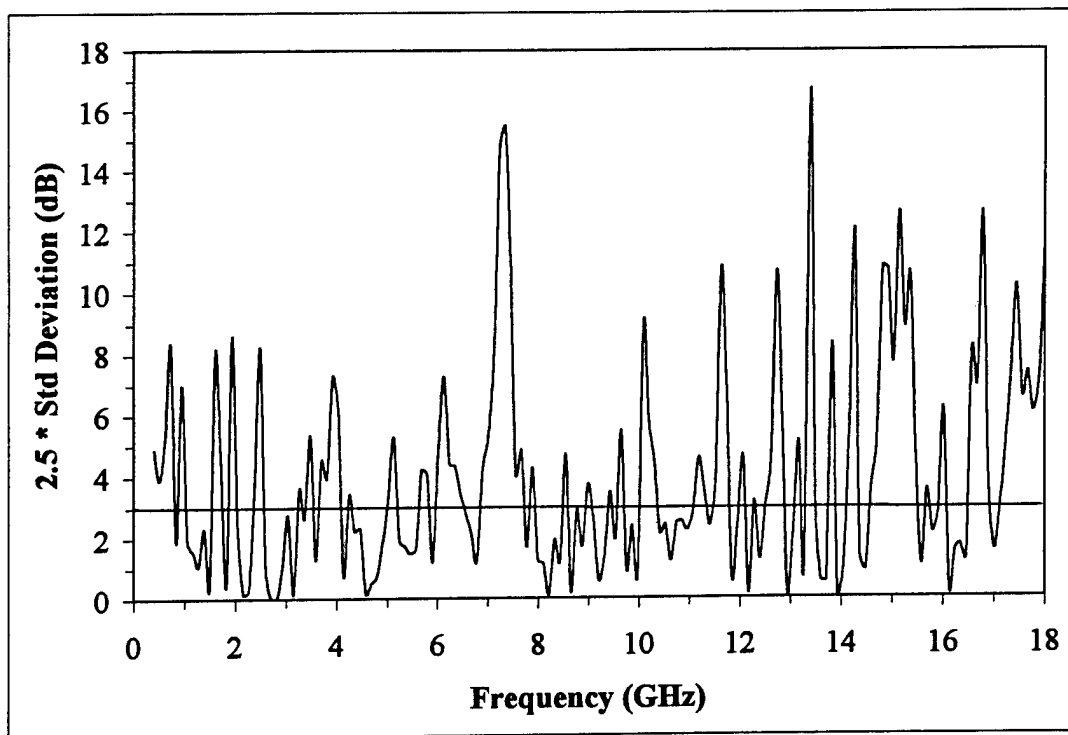


Figure 16: Error Between 2 Probes in the BLWGN Nested Chamber with 100 MHz

The field uniformity measured in the nested chamber using BLWGN was not below the desired 3 dB point, but Figure 12 shows that BLWGN still compared well to the EMSC. It is not understood how the field uniformity of the nested chamber in the anechoic chamber is poor (± 6 dB), yet the BLWGN measurement still compares well with the EMSC measurement.

The source antenna directly illuminated one probe (Probe B as shown in Figure 9), and thus it could not be compared to the other two probes because it measured a higher field level than the average field level in the nested chamber. The source antenna in a reverberation chamber must never directly illuminate probes. Probes must measure the field level resulting from the superposition of waves reverberating in the chamber [5]. This is why the source antenna is always directed into a corner of the reverberation chamber.

4.4.3 Lower Operating Frequency of the Nested Chamber

Figure 15 above shows that the lower operating frequency of the nested chamber was 4 GHz. Neither the 50 MHz NBW, nor the 100 MHz NBW, provided sufficient field uniformity below 4 GHz. The predicted lower operating frequency for a 100 MHz NBW in Section 2.3 was calculated to be 1.5 GHz. This prediction may be lower than the measurement because the prediction was based on the theoretical number of independent modes and not the measured number of independent modes. The measured number of independent modes is based on a measurement of the chamber Q, but this measurement was not made during this experiment. The measured chamber Q can be as much as 60% less than the theoretical chamber Q.

4.5 Error Analysis for Shielding Effectiveness Measurements

The error was calculated by multiplying 2.5 times the standard deviation (with one degree of freedom) [5]. The standard deviation was calculated by

$$s = \sqrt{\frac{(y_a - \bar{y})^2 + (y_b - \bar{y})^2 + (y_c - \bar{y})^2}{n - v}} \quad (14)$$

where y_a is the Probe A measurement, y_b is Probe B, y_c is Probe C, n is the number of measurements ($n=3$), \bar{y} is the sample mean, and ν is the degrees of freedom ($\nu=1$).

There is one degree of freedom because there is one dependent variable in the calculation of the standard deviation. In other words, one of the probe measurements can be determined when the other two measurements, the number of measurements, and the sample mean are known. For example

$$y_c = n\bar{y} - y_a - y_b. \quad (15)$$

The graph of the standard deviation should be $2.5s$ instead of s to show the 99% confidence interval. A field strength of ± 3 dB is equivalent to a $2.5s$ confidence interval. The standard deviation is reported with units of dB.

The goal of a reverberation chamber is for the probes to be no more than 3 dB different. Figure 15 shows that the three probes in the nested chamber in the reverberation chamber differed by more than 3 dB below 4 GHz, around 10 GHz, and above 14 GHz. The probes differed by more than 3 dB at the high and low ends because they were measuring noise and not energy transmitted into the chamber. The large deviation around 10 GHz in the nested chamber is not understood. The large deviation around 9 GHz in the large reverberation chamber is not understood either. Figure 15 shows that there was up to a 3 dB error in the shielding effectiveness measurement due to the non-uniform fields in the nested chamber. Figure 8 shows that the probe measurement was well out of the noise floor above 1 GHz. The large error between 1 GHz and 4 GHz is not due to the measurement being in the noise floor, but rather it is due to the lack of field uniformity in the small volume of the nested chamber.

Figure 14 shows that the three probes in the large chamber differed by more than 3 dB below 2 GHz and around 9 GHz. The probes differed by more than 3 dB at the low end because they were measuring noise and not energy transmitted into the chamber. The large deviation around 9 GHz is not understood. Error measurements in the nested chamber inside the anechoic chamber were about 6 dB between two probes (See Figure 16).

The transition from near field to far field is defined as $2D^2/\lambda$ where D is the maximum dimension of the antenna [3]. The maximum dimension of the antenna was 0.2 m, so the transition point was at 0.3 m at 1 GHz, and it was at 6 m at 18 GHz. The transmitting antenna was in the near-field region for the BLWGN measurements, so this could add some further error to these measurements.

The wave impedance must be constant with frequency and location to convert between the power density (dBm/cm^2) and the field strength (V/m). Ideally, the wave impedance should be the same as free space. The average wave impedance vs. frequency in a reverberation chamber was measured to be close to the wave impedance for free space (377Ω) [8]. Figure 17 below shows a graph of this data.

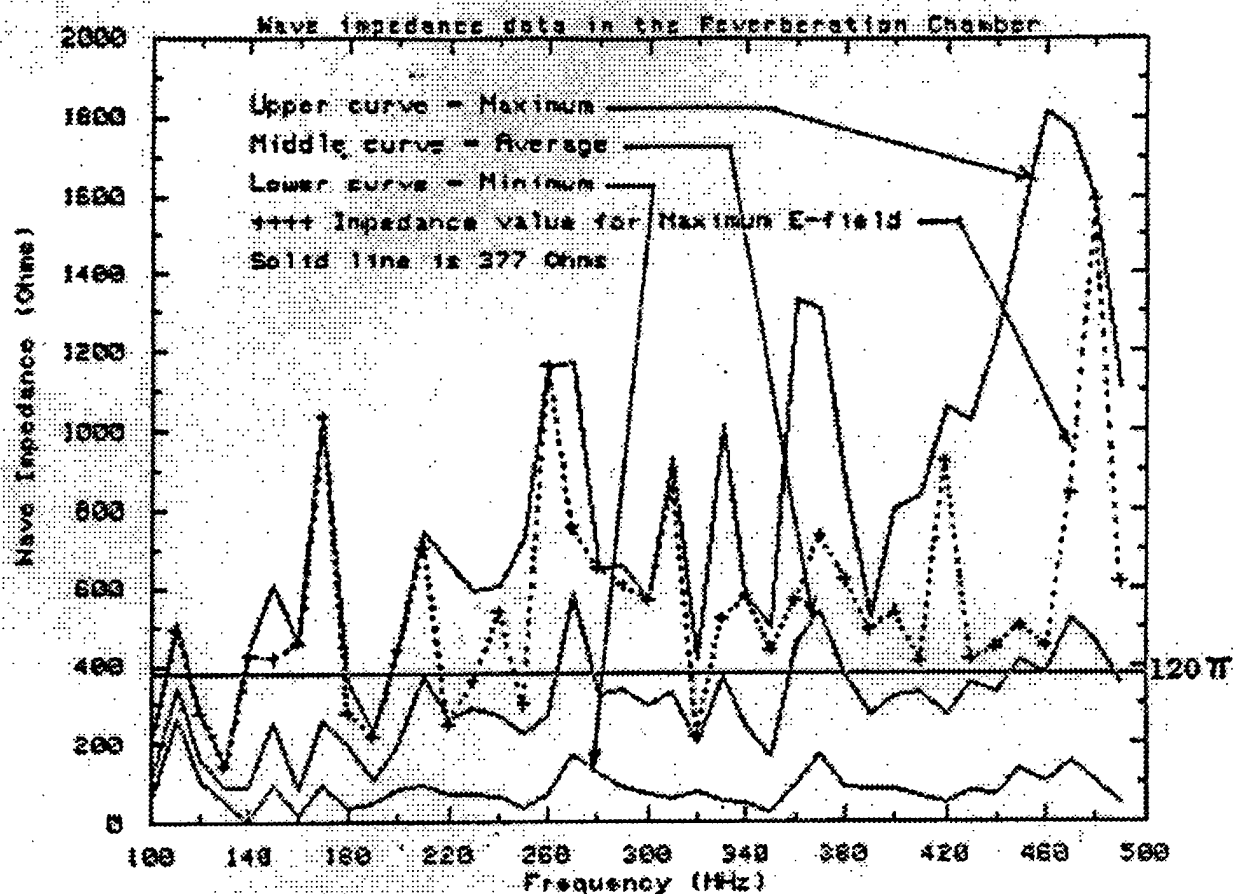


Figure 17: Wave Impedance in a Reverberation Chamber

Although the average wave impedance is close to 377Ω , the variation in wave impedance over frequency translates into an error of ± 2 dB in a field measurement.

The overall error associated with the EMSC measurements was ± 5 dB above 4 GHz and below 14 GHz. The error was larger from 400 MHz to 4 GHz and from 14 GHz to 18 GHz, since the measurements were approaching the noise floor in these areas (See Figure 8). The overall error associated with the BLWGN measurements was ± 8 dB.

In the future, measurements of the noise from the TWTs, and the VSWR from the transmit antenna and receive antenna should be taken so that a more thorough error analysis. Also the probes should be characterized to determine their actual (not predicted) sensitivity and precision from 400 MHz to 18 GHz. Also, the nested chamber should not be used for measurements below 4 GHz.

4.6 IR Transmission Measurements

The IR transmission for the thin film could not be determined (Figure 18).

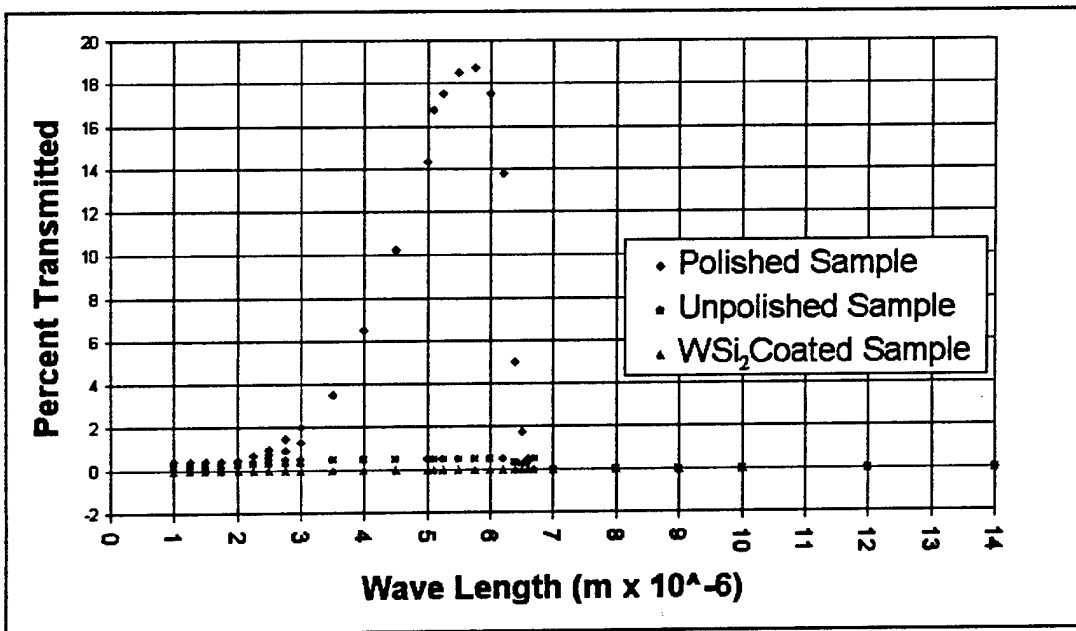


Figure 18. IR Transmission Measurements

The IR transmission for the thin film could not be determined. The polished substrate transmitted 20% IR around 6 μ m and transmitted 0% at all other wavelengths. The unpolished substrate and thin film window did not transmit IR at any of the wavelengths measured. The thin film window did not transmit IR around 1 μ m and between 8 – 12 μ m because the polished substrate did not transmit IR in these

wavelengths. (The thin film was sputtered onto the polished substrate and was then called a thin film window.) IR transmission at $6\text{ }\mu\text{m}$ would not imply IR transmission between $8 - 12\text{ }\mu\text{m}$, so the IR transmission of the thin film window remains undetermined.

5.0 Conclusions

The measured shielding effectiveness of the thin film was 25 dB from 4 GHz to 12 GHz based on the EMSC and BLWGN measurements. Angle of incidence information could not be obtained from the BLWGN measurements because the TWTAs did not provide enough power at a sufficient distance. The predicted shielding effectiveness was 29 dB, and the error analysis shows that this predicted value was within the measurement error of the experiment. The polished substrate was also measured, and it did not contribute to the shielding effectiveness of the thin film window. The measurements were not made below 4 GHz due to a lack of field uniformity in the nested chamber. Measurements were not made above 12 GHz because of a combination of using the B-dot probes outside their accurate range and insufficient power to keep the measurements out of the noise floor. Shielding effectiveness measurements should not be conducted below 4 GHz with the nested chamber. This is because less than 3 dB of field uniformity cannot be maintained in the nested chamber below 4 GHz, and large measurement errors will result.

The shielding effectiveness prediction was based on the shielding effectiveness due to reflection not absorption. Reflection dominated the shielding effectiveness because the film thickness was less than its skin depth. The film thickness had no effect on the RF shielding effectiveness of the thin film window, so the film should be made as thin as possible to maximize IR transmission.

The IR transmission could not be determined because the substrate did not transmit IR at the required wavelengths. A different and inexpensive substrate that transmits IR at the required wavelengths will be used in the future. A zinc-sulfide substrate will be used in the final thin film window, but it is too expensive to use for research purposes. Research showed that the thin film material selected could transmit up to 90% IR, and IR measurements of similar materials showed that a transmission of 60 to 70% should be expected.

6.0 Recommendations

The standard approach to shielding effectiveness measurements are MIL-STD-285, the Coaxial Holder Method (American Society for Testing Materials), the Dual-Chamber Method (American Society for Testing Materials), and the Dual TEM Cell Method. MIL-STD-285 should be used in a future experiment to measure the shielding effectiveness of the thin film to verify the shielding effectiveness and further validate the EMSC technique.

Note that MIL-STD-285 is not an ideal measurement technique. The presence or absence of a conductive window affects the interaction of the wall that separates the transmission from the measurement probe. There is a discontinuity (hole) in the wall without the window, and continuity in the wall with the window; the wall will shield the transmission differently in each of these cases. The advantages and disadvantages of every technique must be taken into account.

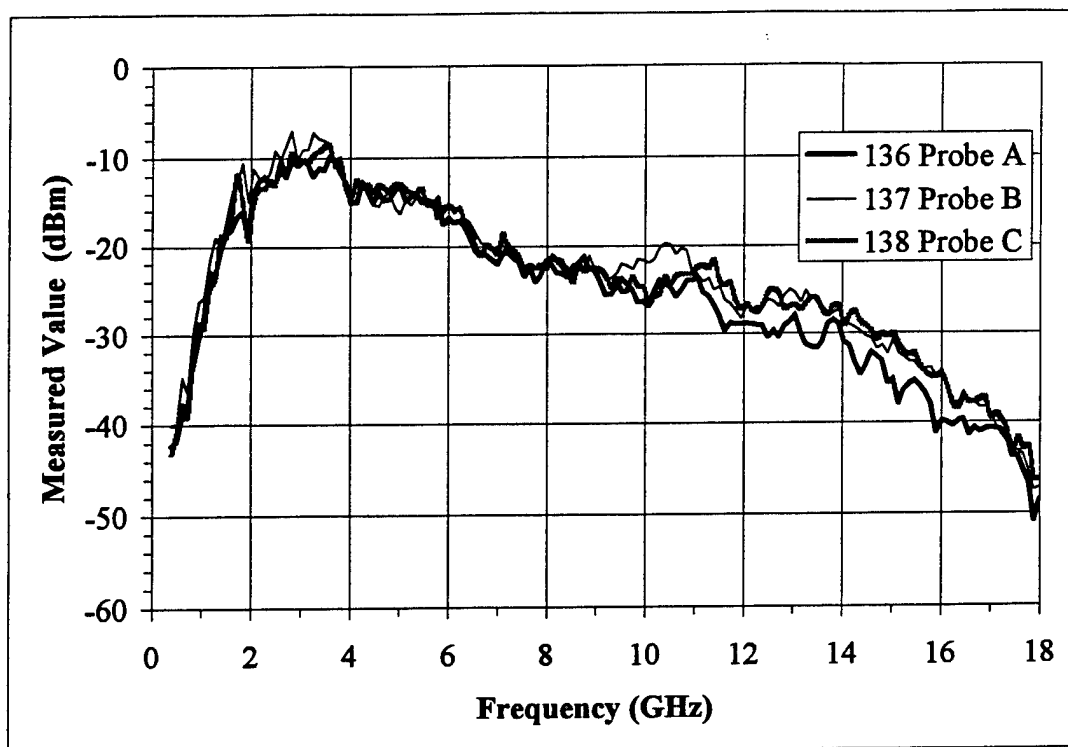
The chamber Q should be measured to better predict the lower operating frequency of the nested chamber. Further, 200-Watt TWTAs should be used to provide sufficient dynamic range to characterize the thin film window, and also reconfirm the lower operating frequency of the nested chamber. More analysis should be done to understand how to predict the shielding effectiveness through a 0.1 m aperture, and understand why the nested chamber aperture shields more than the calculated value. Further, measurements should be made of the noise from the TWTs, and the VSWR from the transmit antenna and receive antenna in order to more carefully characterize the errors associated with the measurement. The field uniformity of the nested chamber inside an anechoic chamber should be further investigated. Finally, the nested chamber should not be used for measurements below 4 GHz to maintain sufficient field uniformity, and a smaller B-dot probe or small horn probe should be used above 12 GHz to use probes in their proper range.

7.0 References

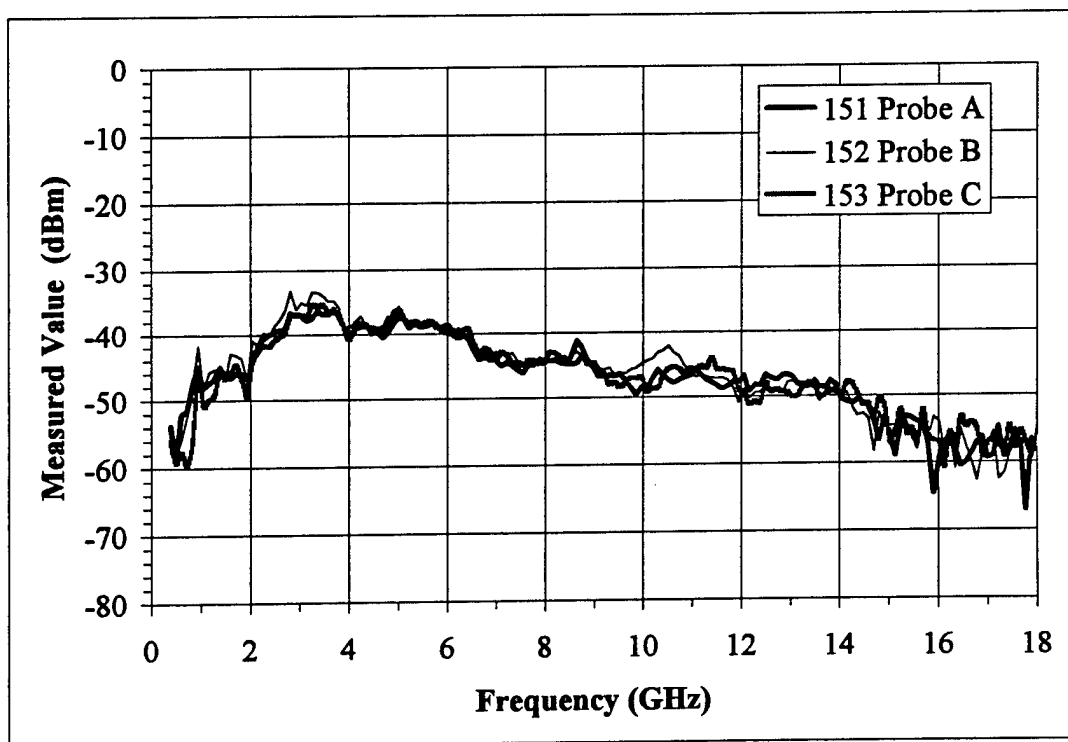
- [1] Savrun, E. *Electrically Conductive Metal Silicides and Ceramics for EMI/RFI Shielding of IR Windows*. Phillips Laboratory, Kirtland AFB, NM, PL-TR-95-1150, Nov., 1996.
- [2] White, R.J., and Mardiguian, M. *Electromagnetic Shielding: Volume 3*. Interface Control Technologies, Inc., Gainesville, VA, 1988.
- [3] Pozar, D.M. *Microwave Engineering*. Addison-Wesley Publishing Co., Reading, MA, 1990.
- [4] Loughry, T.A., and Gurbaxani, S.H. "The Effects of Intrinsic Test Fixture Isolation on Material Shielding Effectiveness Measurements Using Nested Mode-Stirred Chambers," *IEEE Trans. Electromagn. Compat.*, Vol. 37, No. 3, pgs. 449-452, 1995.
- [5] Loughry, T.A. Frequency Stirring: An Alternative Approach to Mechanical Mode-Stirring for the Conduct of Electromagnetic Susceptibility Testing, PL-TR-91-1036, Nov., 1991.
- [6] Antonov, V.N., Jepsen, O., Anderson, O.K., Borghesi, A., Basio, C., Marabelli, F., Piaggi, A., Guizetti, G., and Nava, F. "Optical Properties of WSi_2 ," *Physical Review B*, Vol. 44, p. 8437, 1991.
- [7] Hatfield, M.O. "Shielding Effectiveness Measurements Using Mode-Stirred Chambers: A Comparison of Two Approaches," *IEEE Trans. Electromagn. Compat.*, Vol. 30, No. 3, pgs. 229-238, August 1988.
- [8] Crawford, M.L. and Koepke, G.H. *Design, Evaluation, and Use of a Reverberation Chamber for Performing Electromagnetic Susceptibility/ Vulnerability Measurements*. National Bureau of Standards (U.S.A.). NBS Tech. Note 1092, April 1986.

Appendix A: Graphs

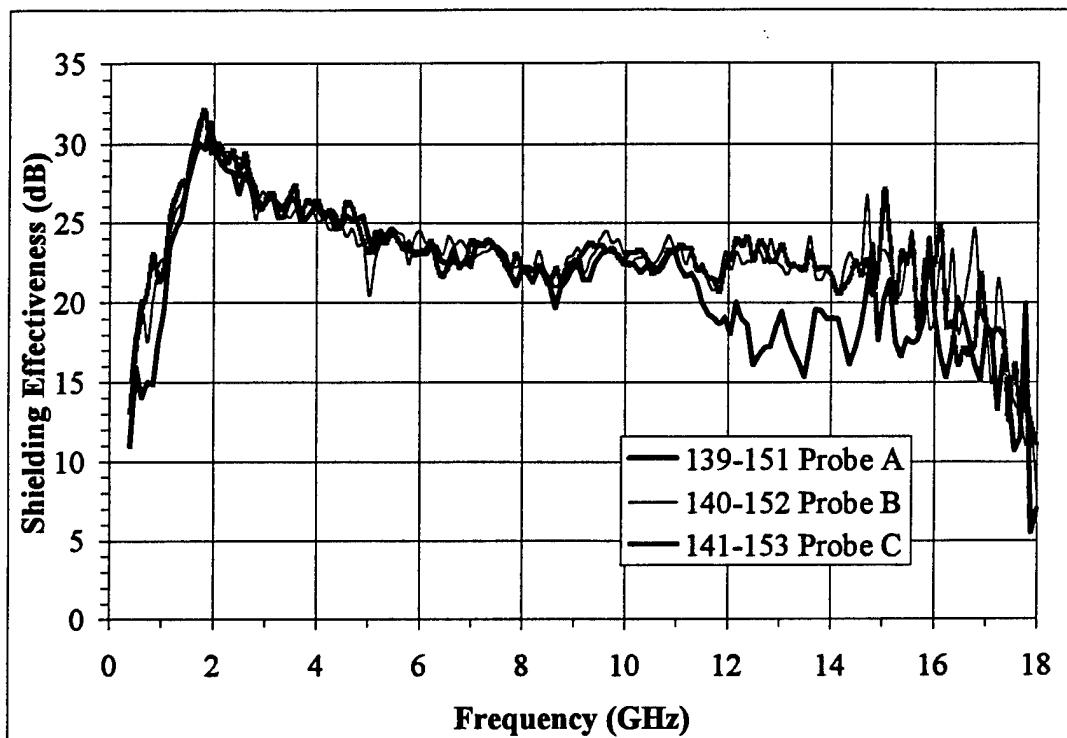
The following is a comprehensive set of graphs from the experiment.



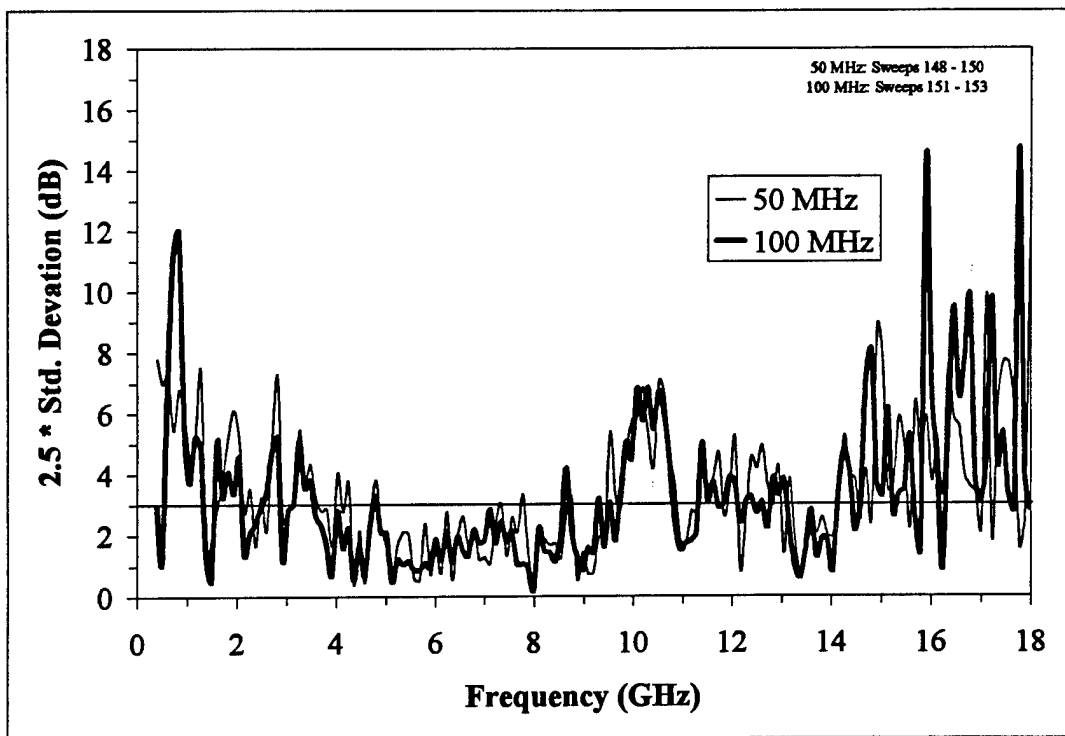
Thin Film in EMSC with 50 MHz: Raw Data



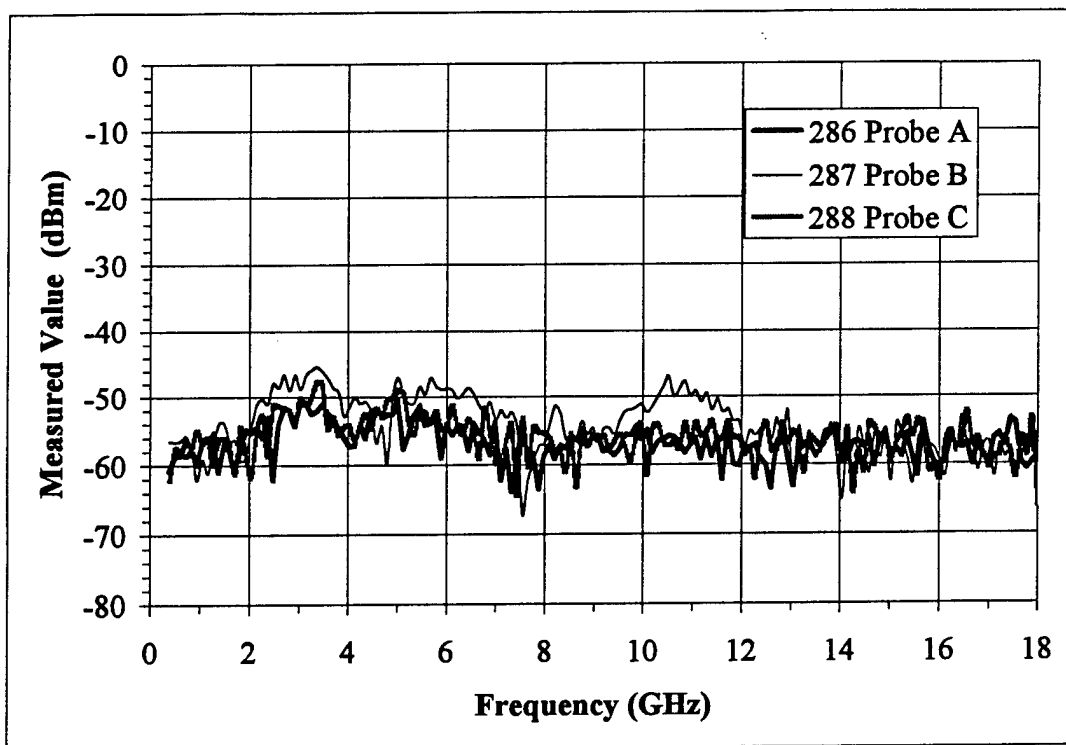
Thin Film in EMSC with 100 MHz: Raw Data



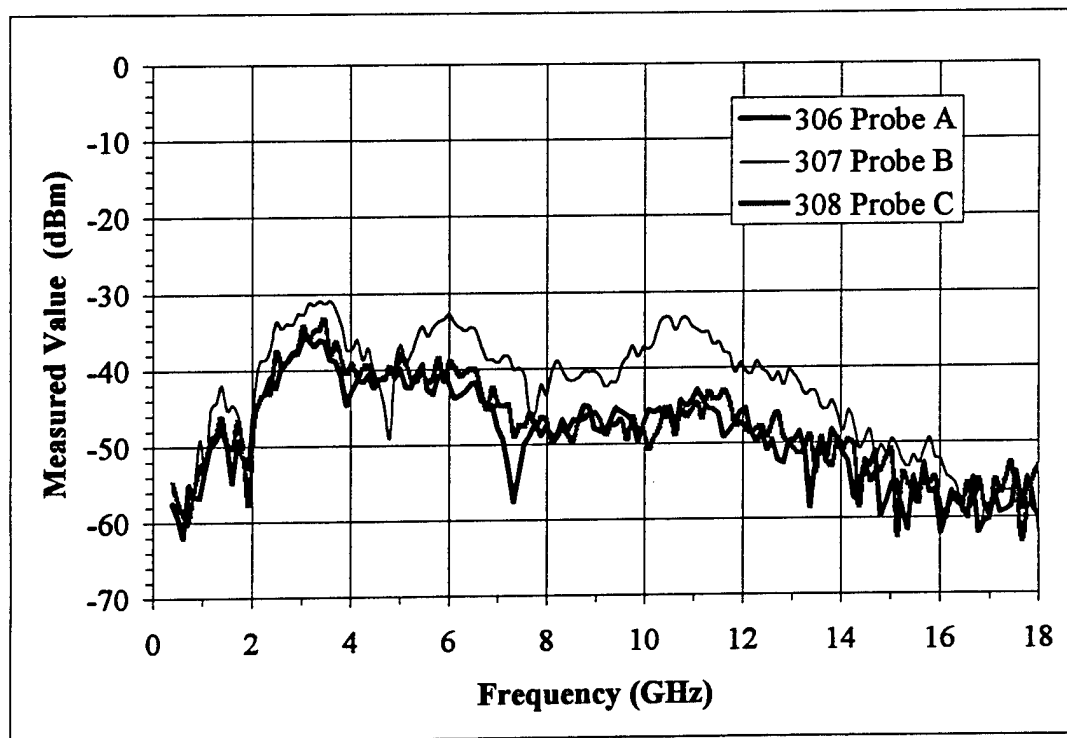
Thin Film in EMSC with 100 MHz: Shielding Effectiveness



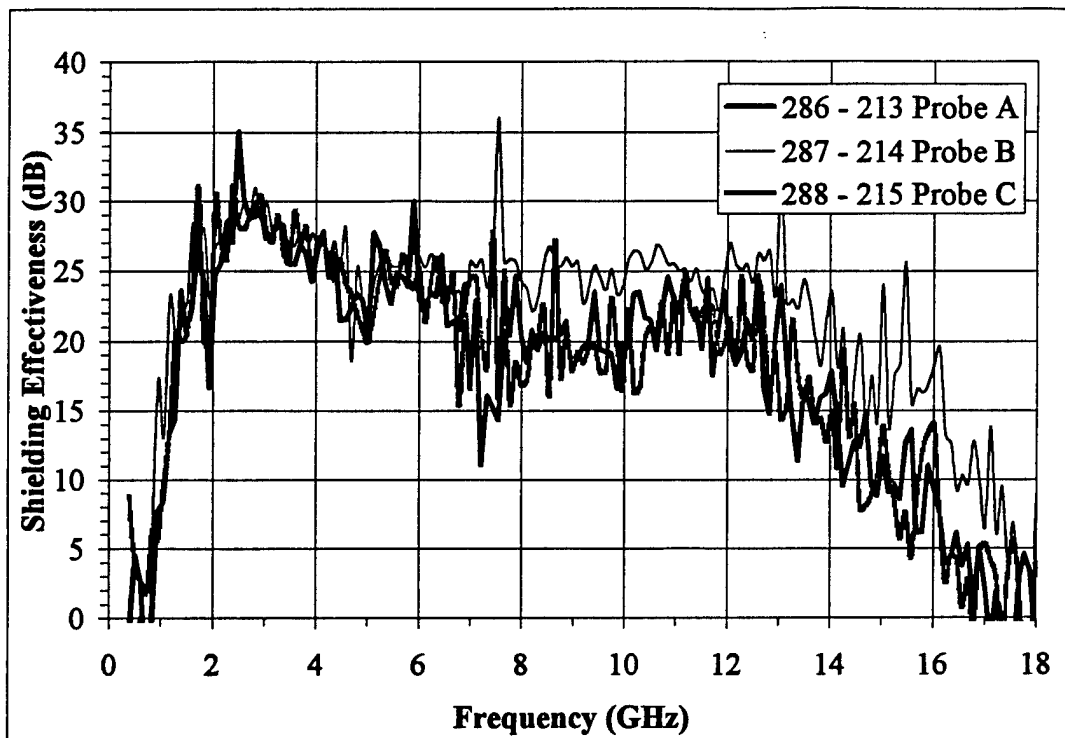
Thin Film in EMSC with 50 and 100 MHz: Error Among 3 Probes



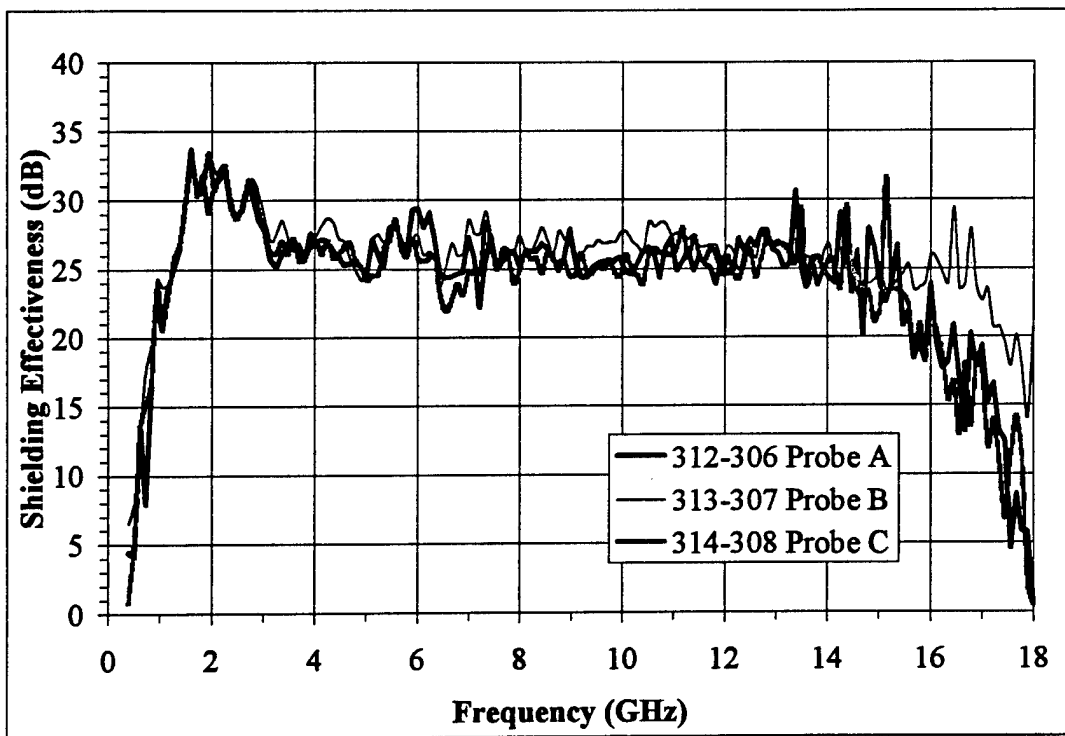
Thin Film with BLWGN and 100 MHz: Raw Data at 5'5" and 0° Incidence



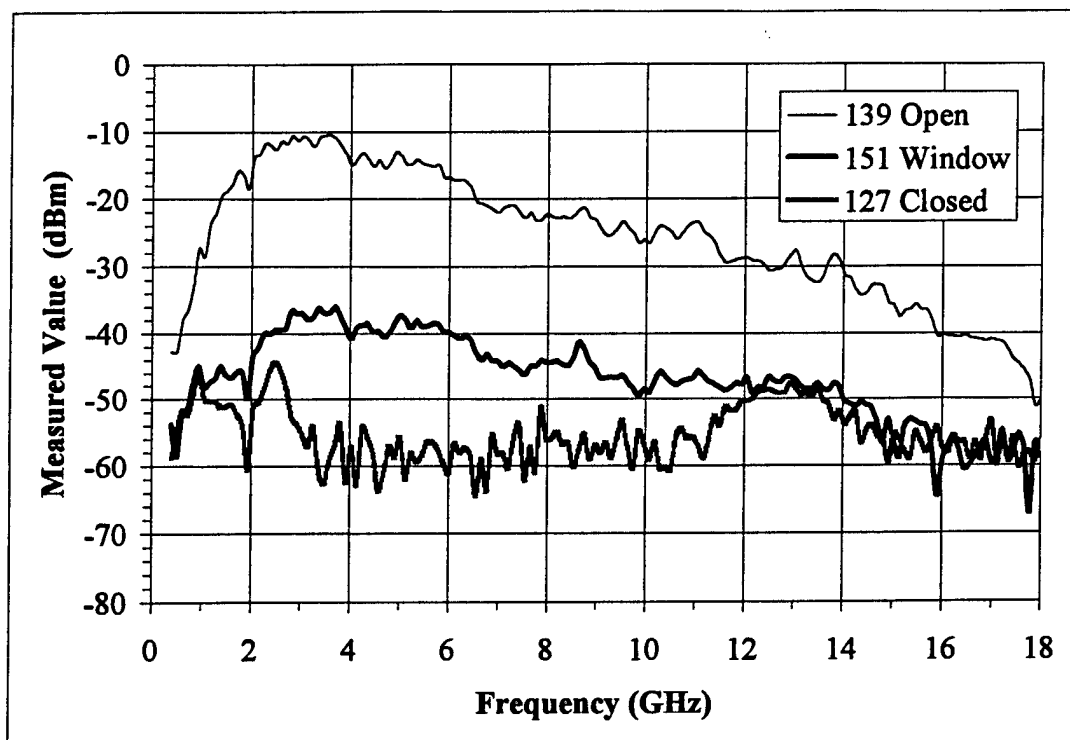
Thin Film with BLWGN and 100 MHz: Raw Data at 9" and 0° Incidence



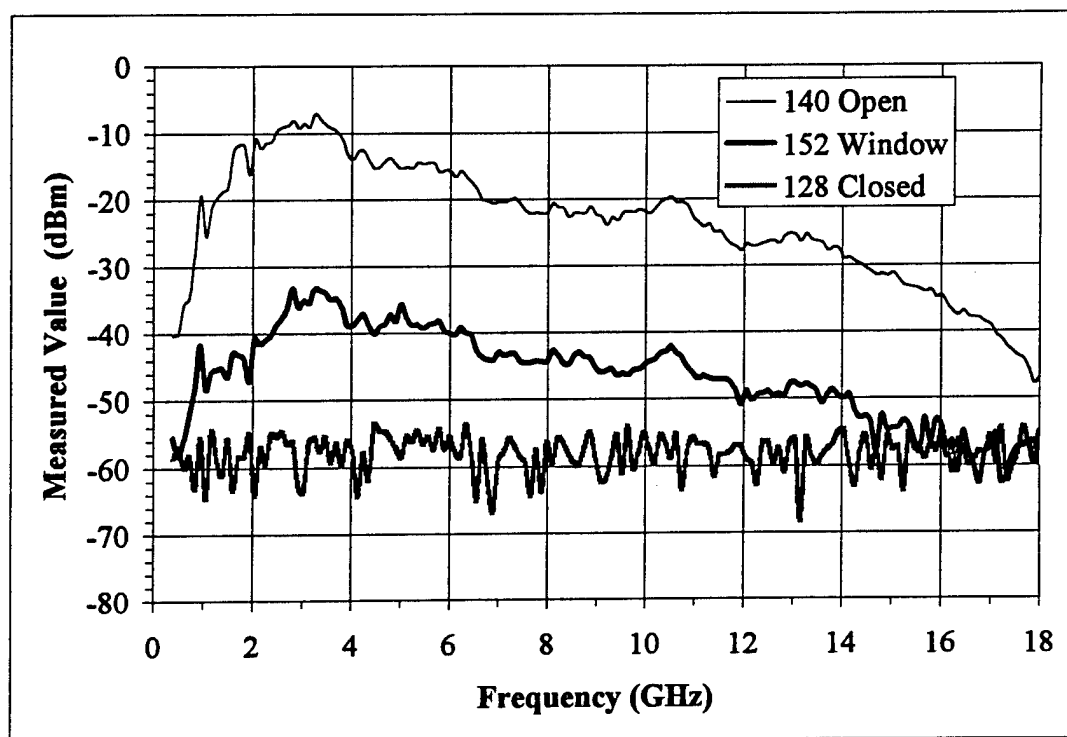
Thin Film with BLWGN, 100 MHz: Shielding Effectiveness at 5'5", 0° Incidence



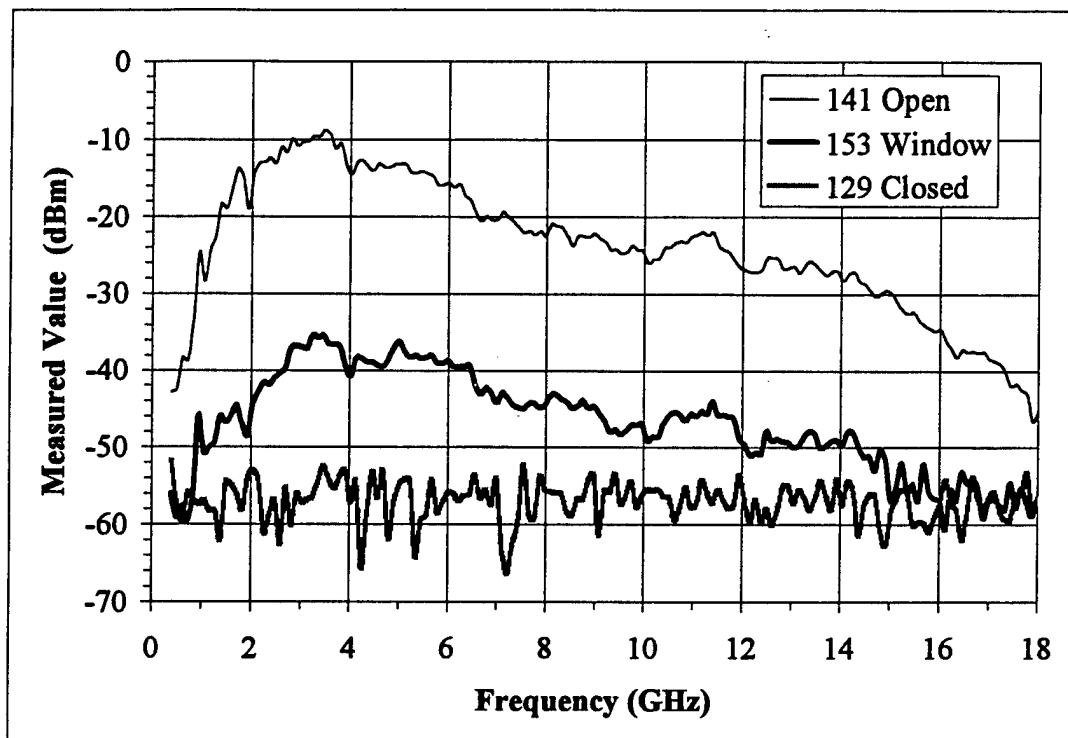
Thin Film with BLWGN and 100 MHz: Shielding Effectiveness at 9", 0° Incidence



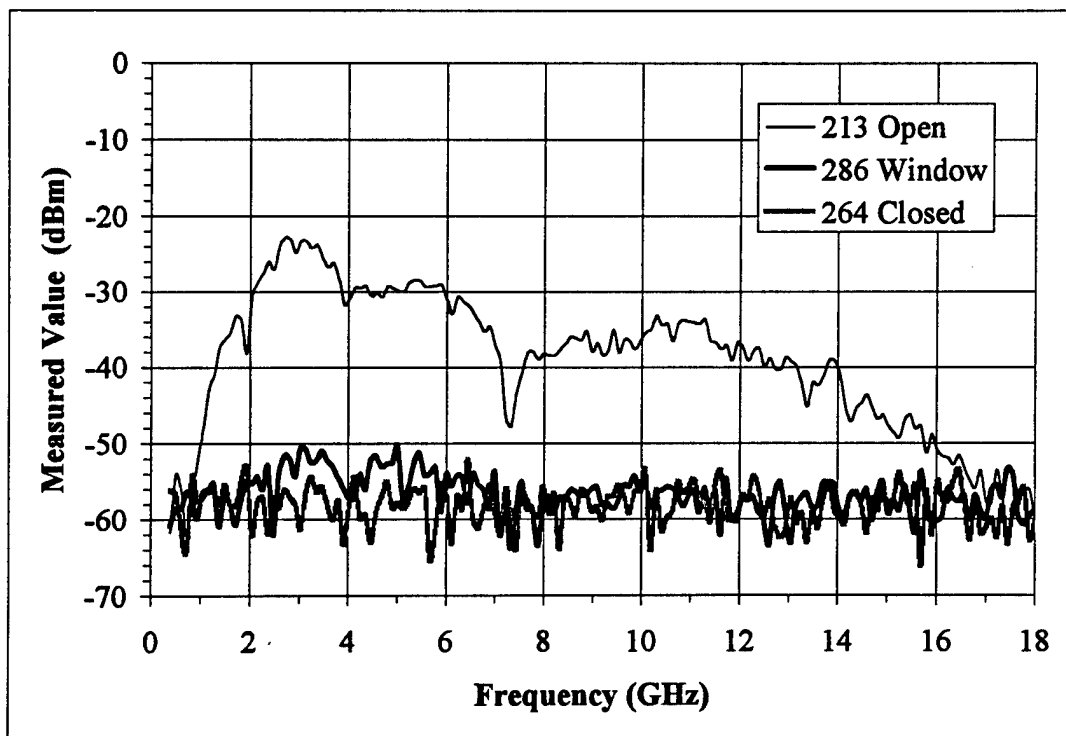
EMSC with 100 MHz: Raw Data for Probe A



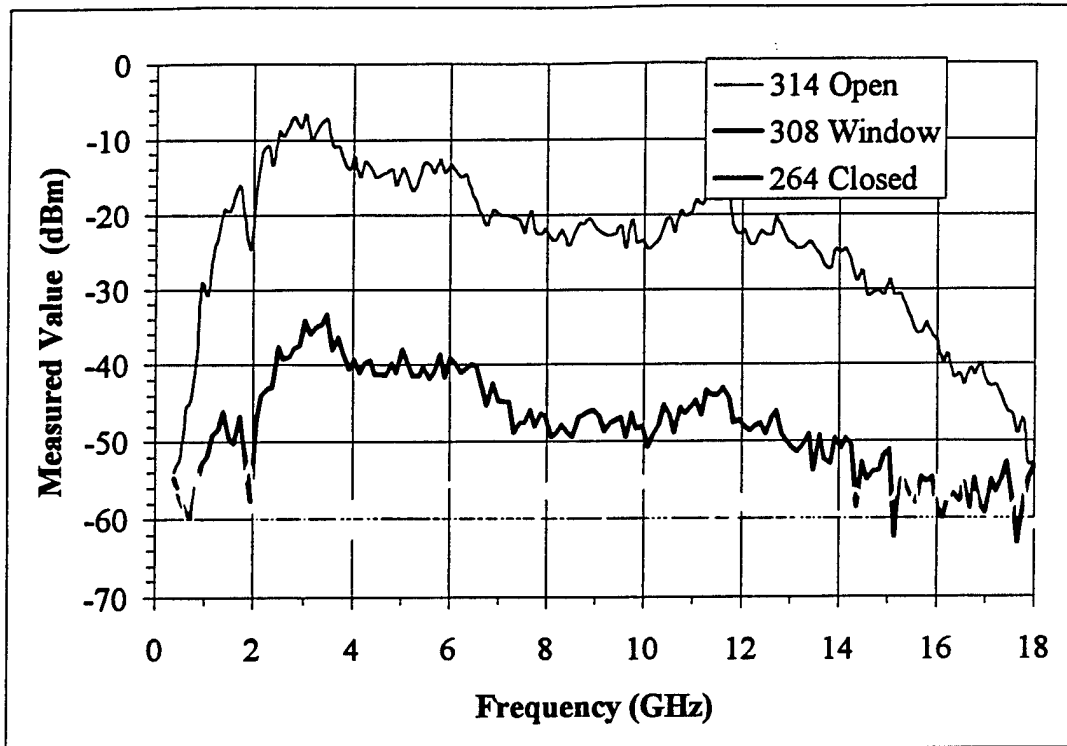
EMSC with 100 MHz: Raw Data for Probe B



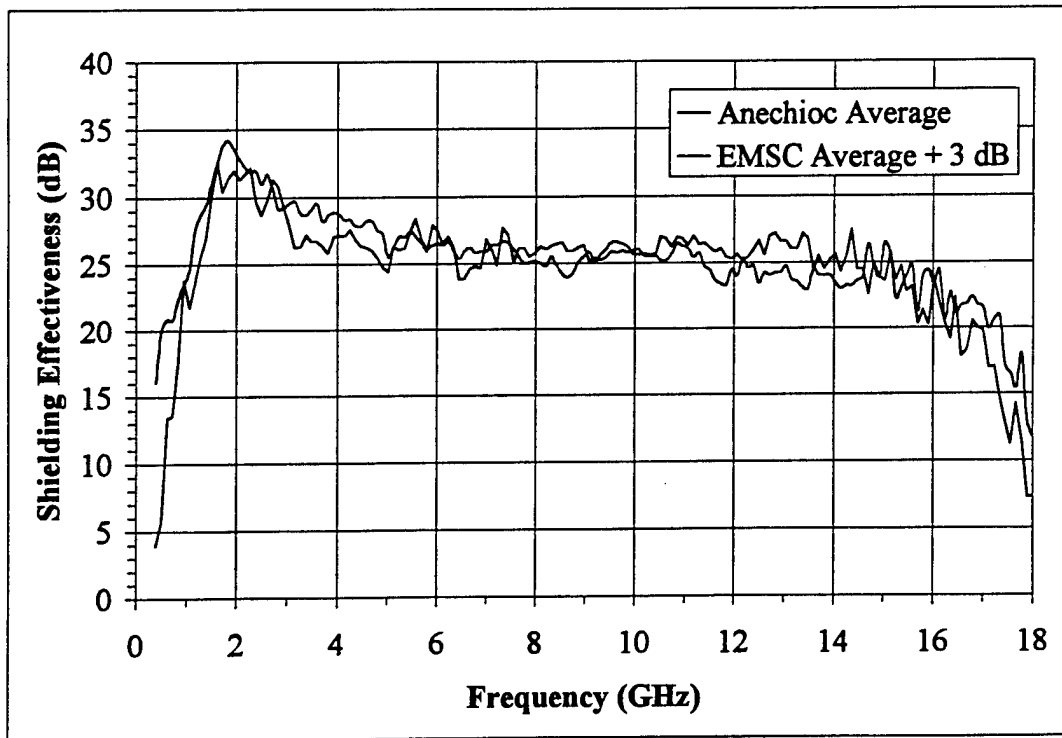
EMSC with 100 MHz: Raw Data for Probe C



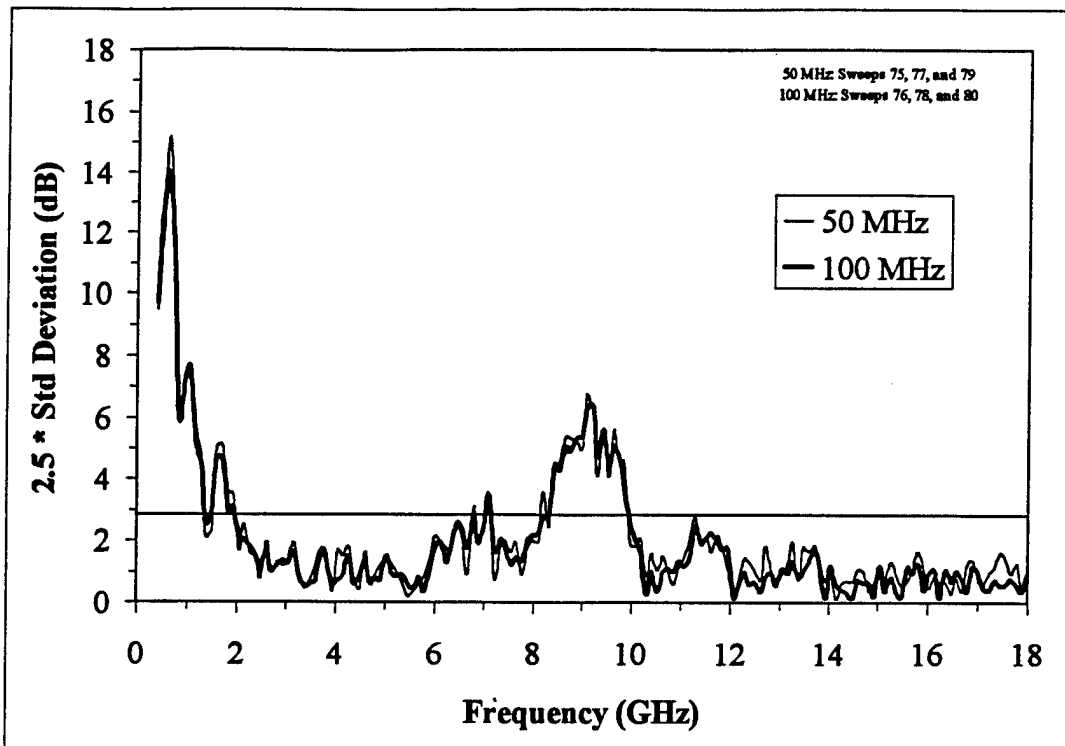
BLWGN with 100 MHz: Raw Data for Probe A at 0° Incidence, 5'5"



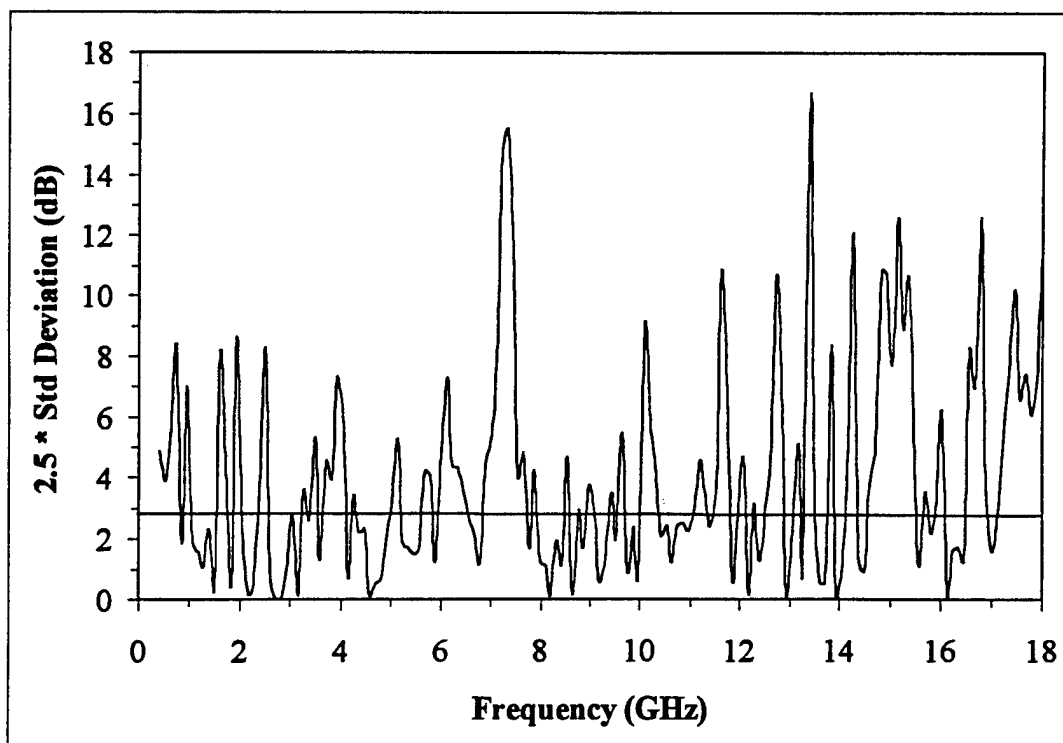
Thin Film with BLWGN: Open, Probe C, and Closed at 9°, 0° Incidence



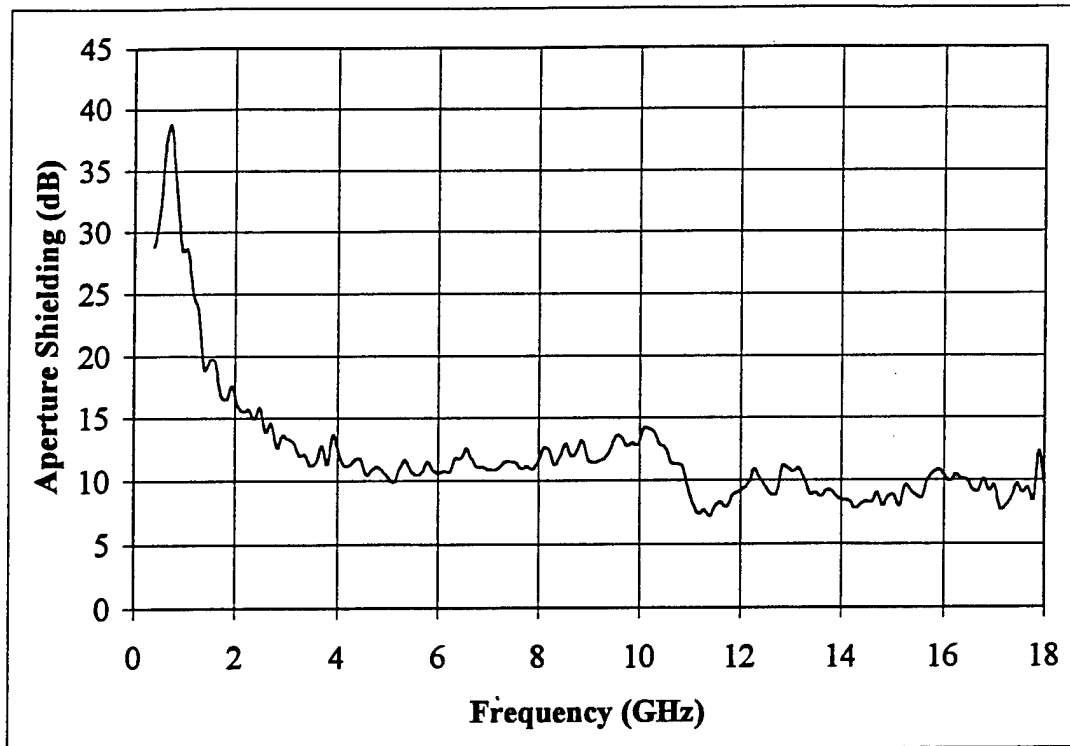
Thin Film Comparison of EMSC to BLWGN



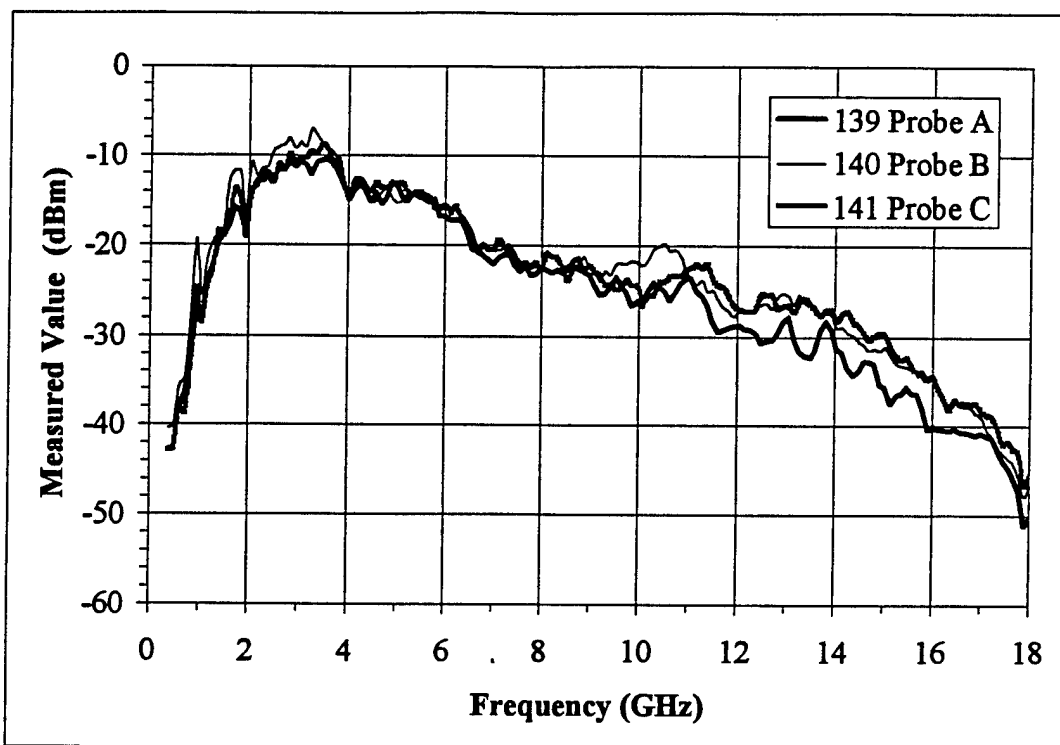
Error Among 3 Probes in Large Reverberation Chamber with 50 and 100 MHz



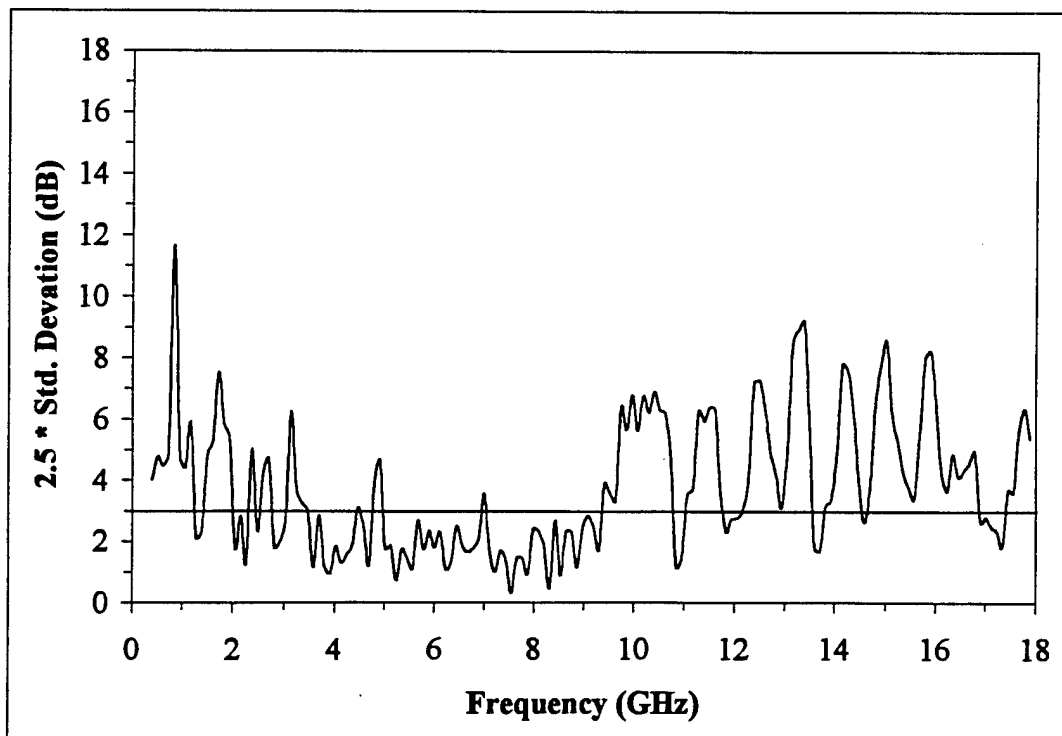
Error Between 2 Probes in Nested Chamber with BLWGN 100 MHz, 9"



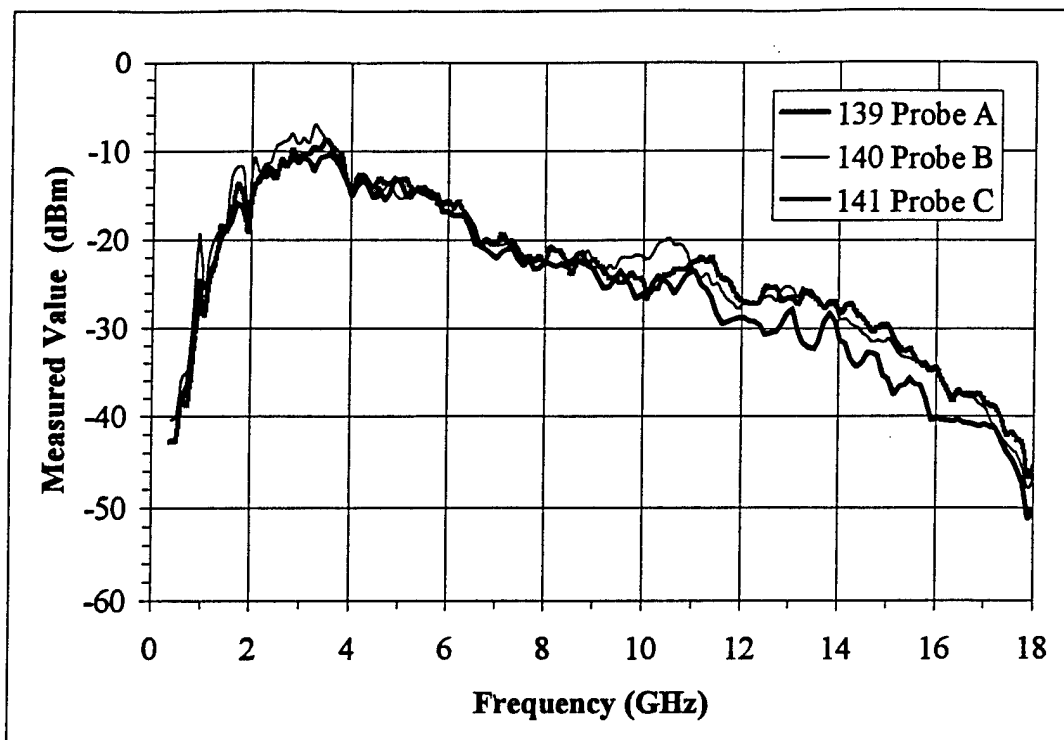
Isolation from Large Reverberation Chamber to Nested Chamber



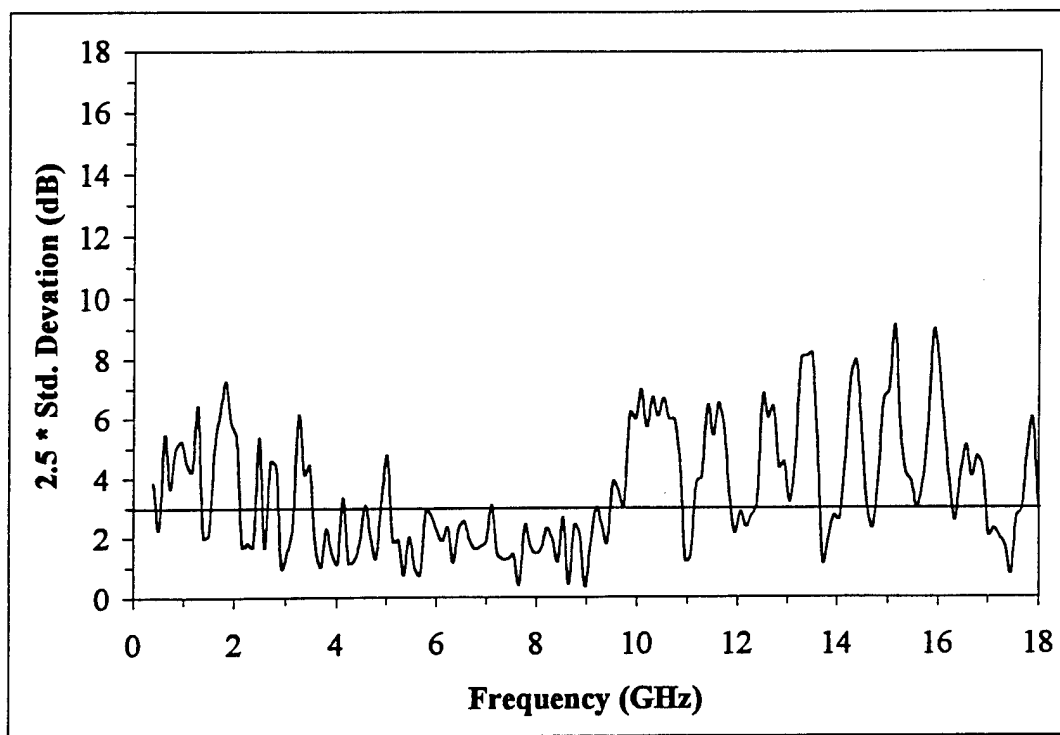
Open Aperture in EMSC with 100 MHz



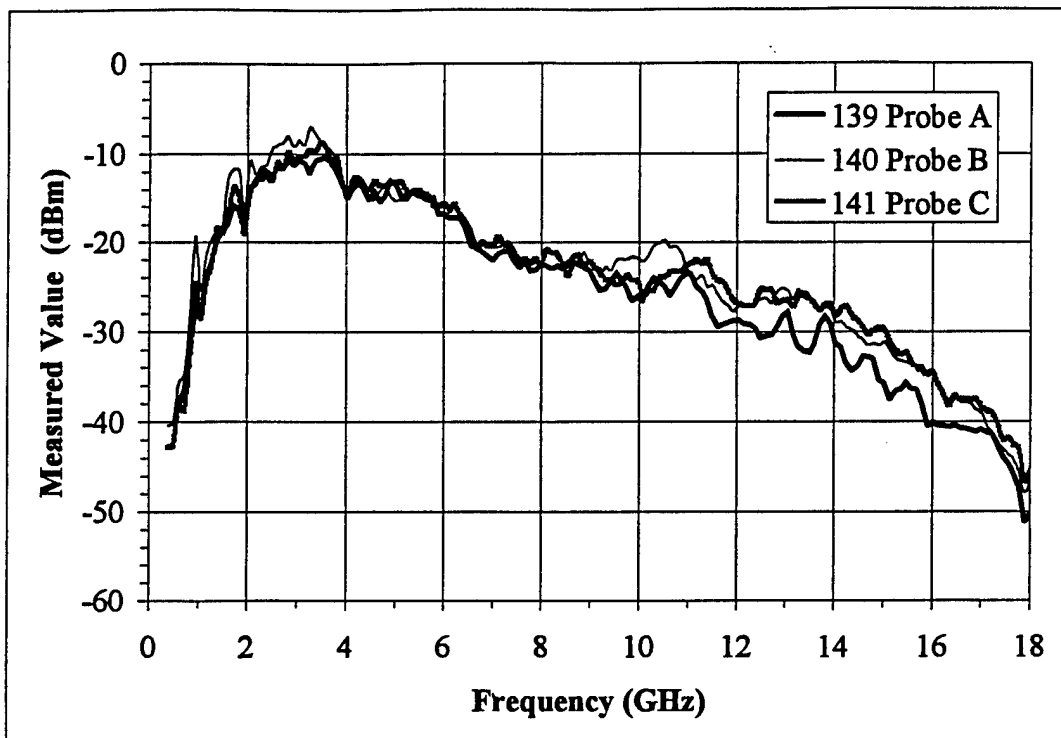
Open Aperture in EMSC with 100 MHz: Error Among 3 Probes



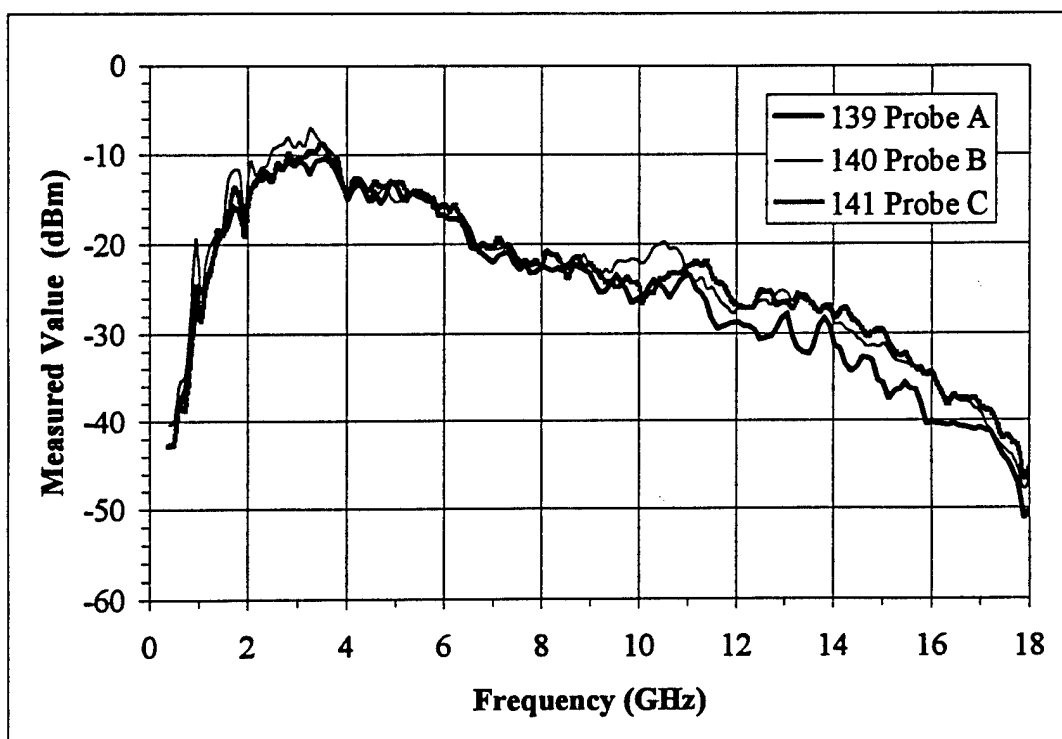
Open Aperture in EMSC with 50 MHz: Raw Data



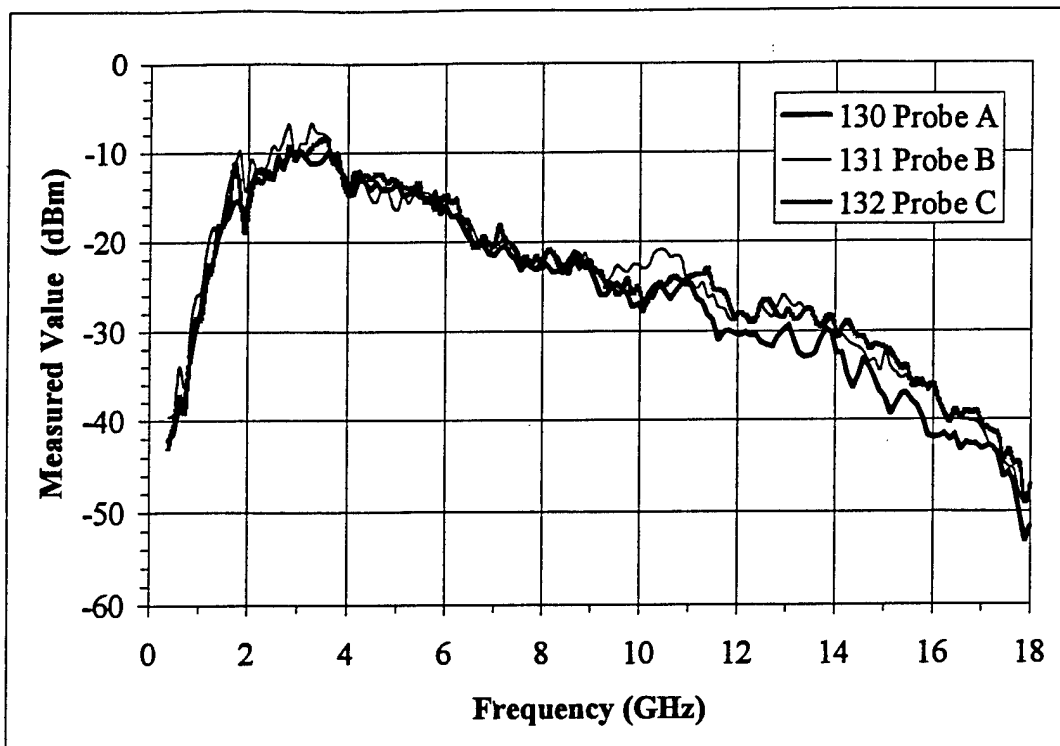
Open Aperture in EMSC with 50 MHz: Error Among 3 Probes



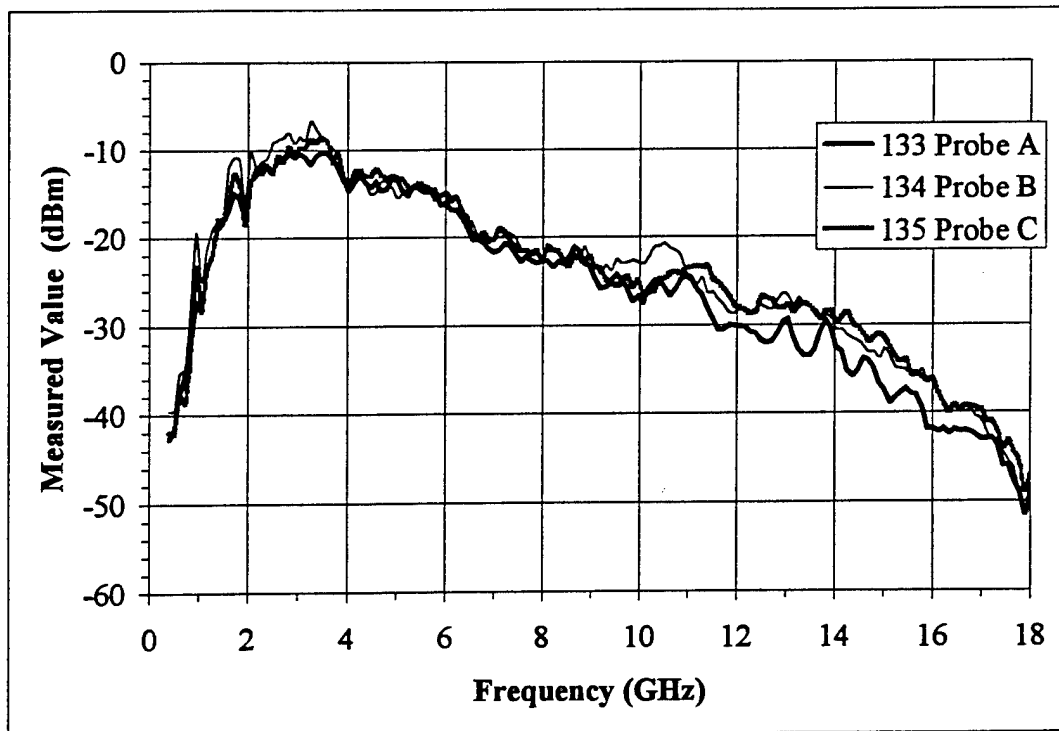
Open Aperture with BLWGN and 100 MHz: Raw Data



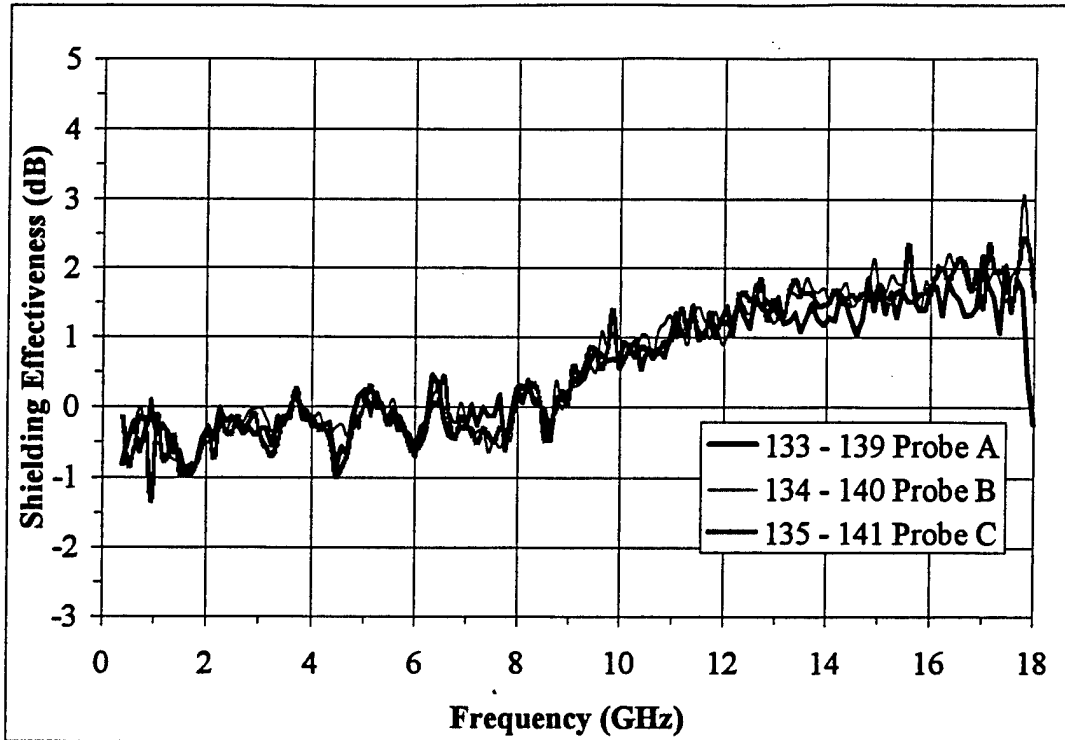
Open Aperture with BLWGN and 100 MHz: Error Among 3 Probes



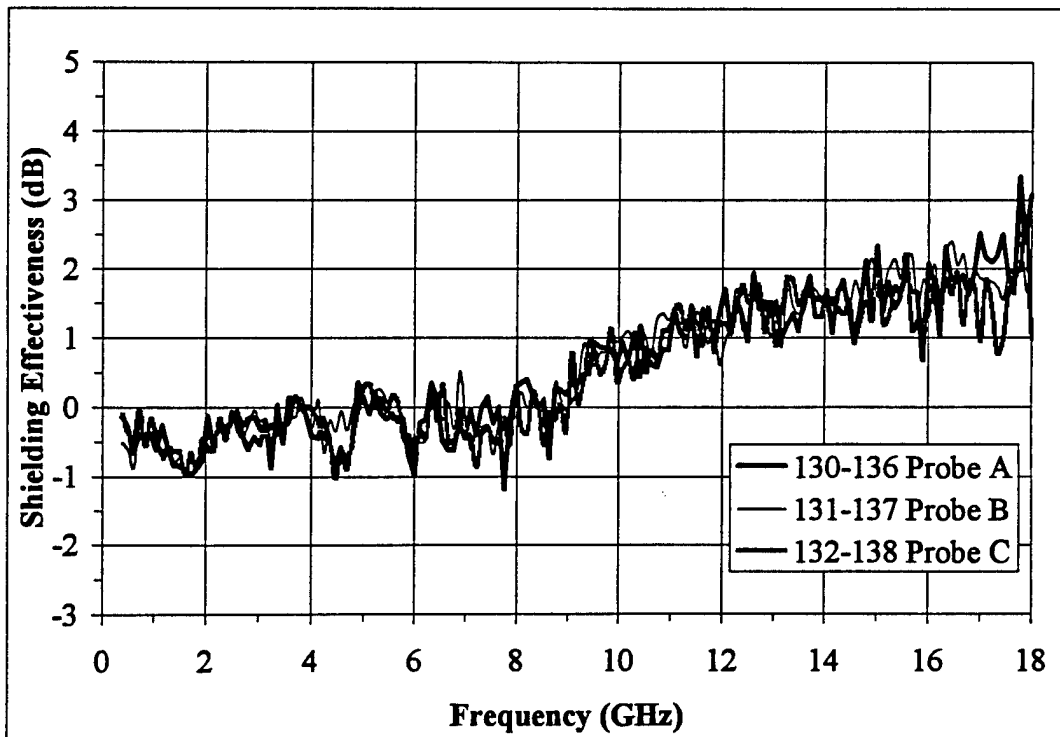
Polished Substrate in EMSC with 50 MHz: Raw Data



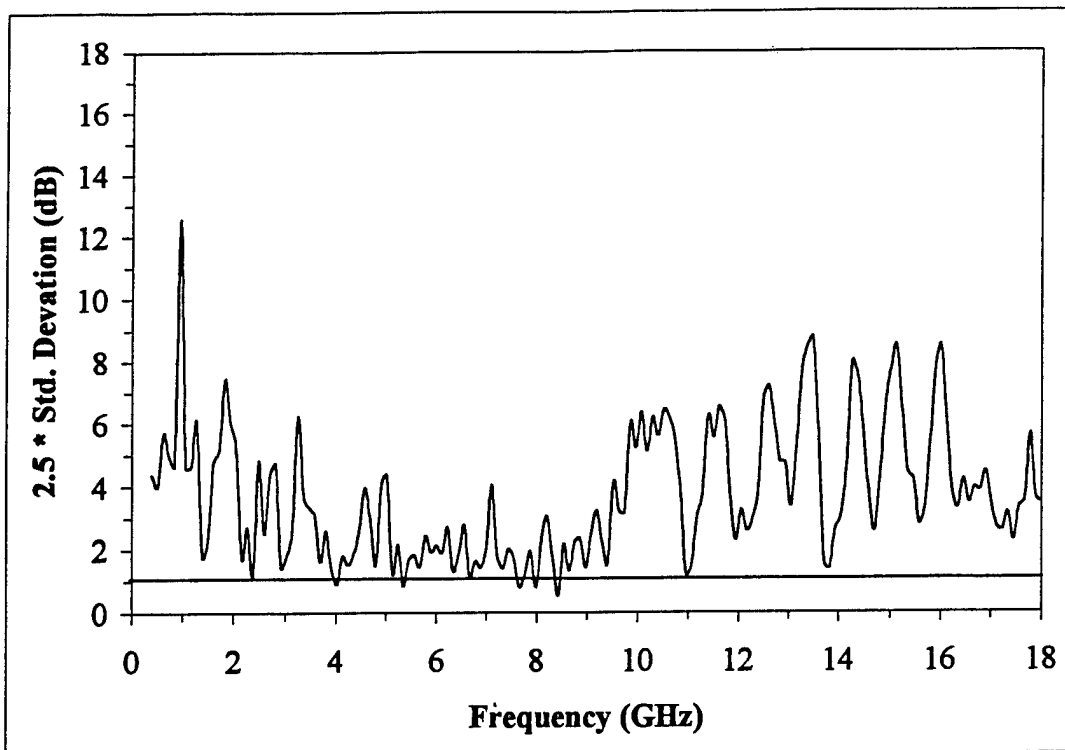
Polished Substrate in EMSC with 100 MHz: Raw Data



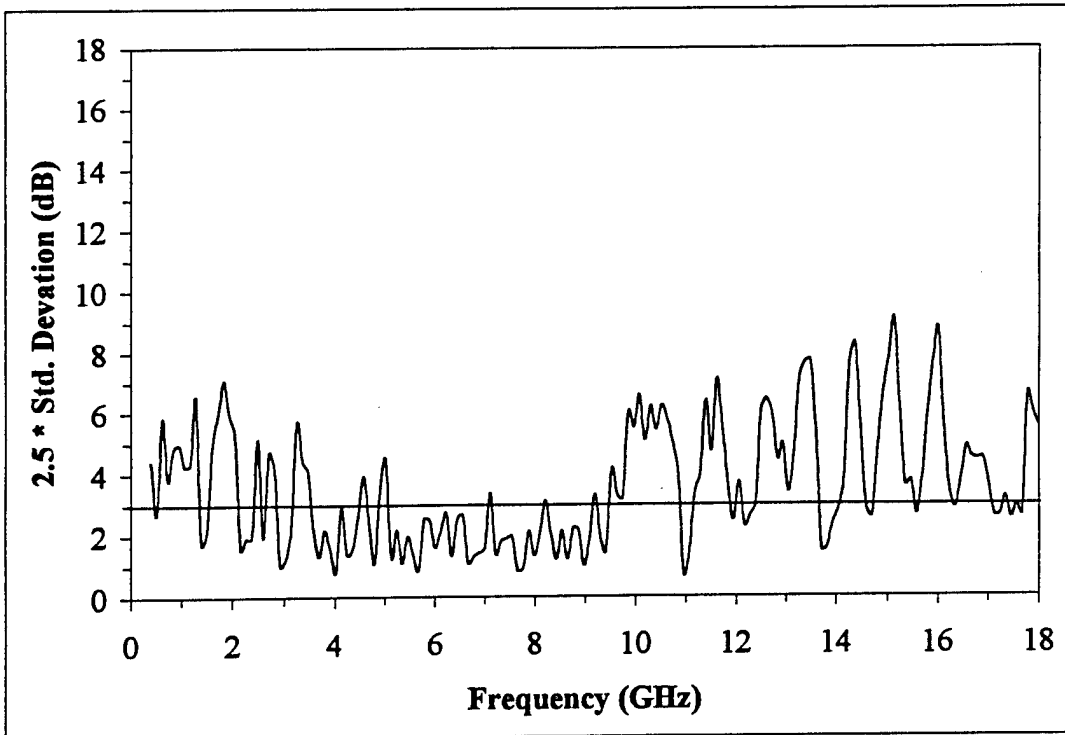
Polished Substrate in EMSC with 100 MHz: Shielding Effectiveness



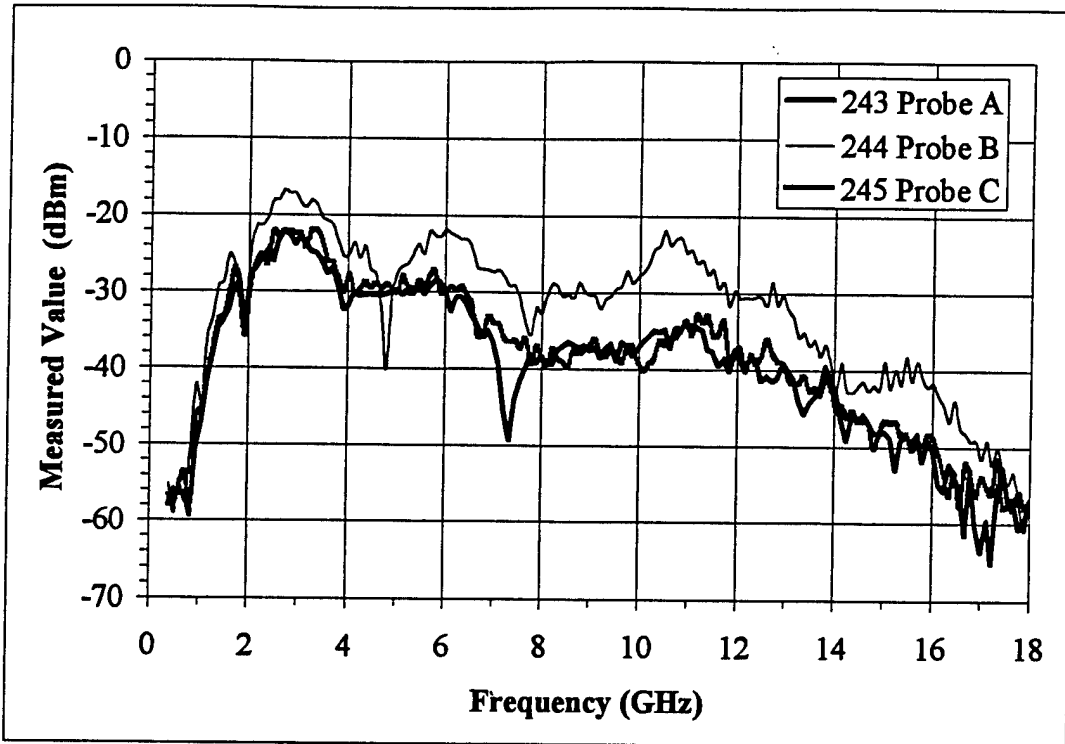
Polished Substrate in EMSC with 50 MHz: Shielding Effectiveness



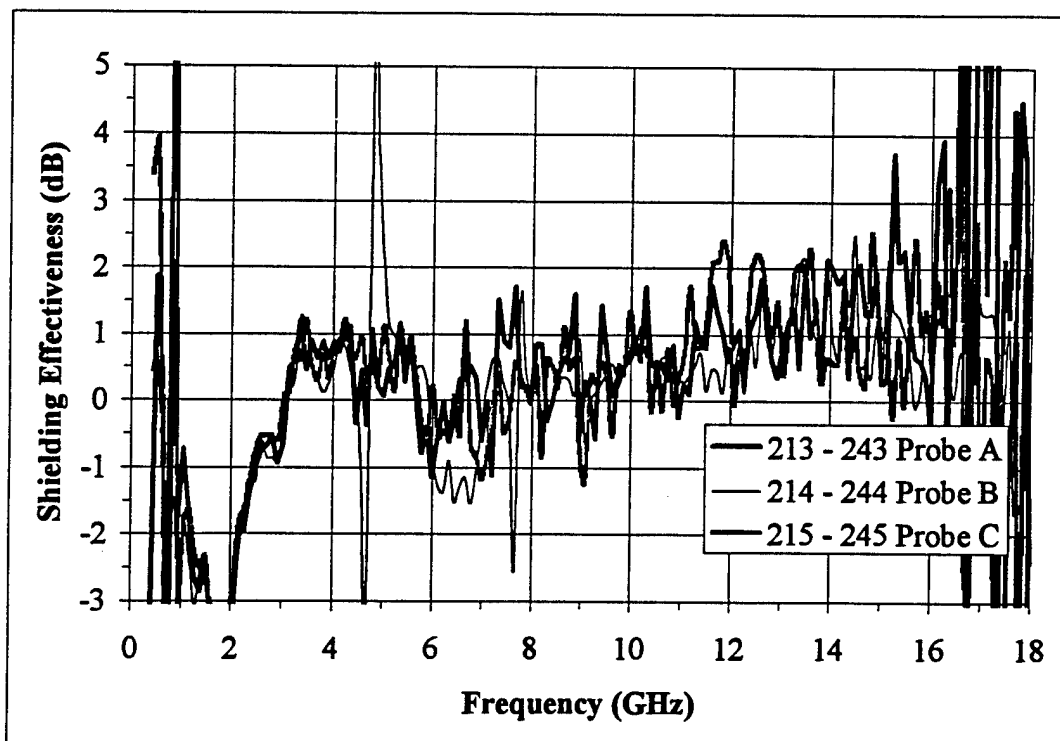
Polished Substrate in EMSC with 100 MHz: Error Among 3 Probes



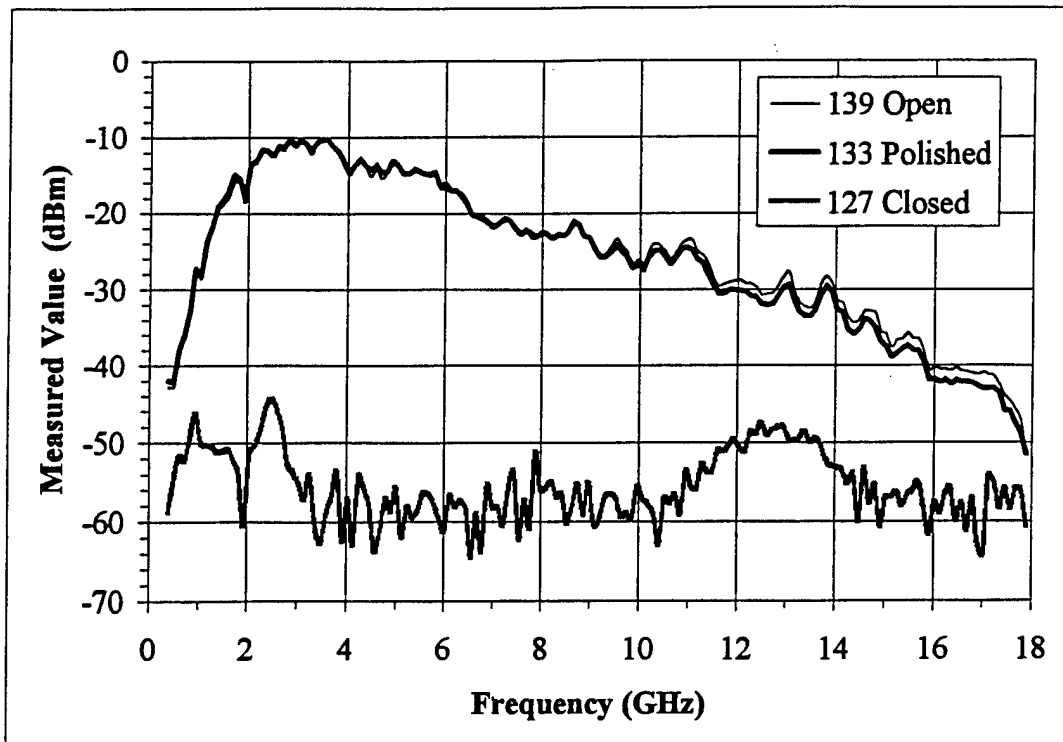
Polished Substrate in EMSC with 50 MHz: Error Among 3 Probes



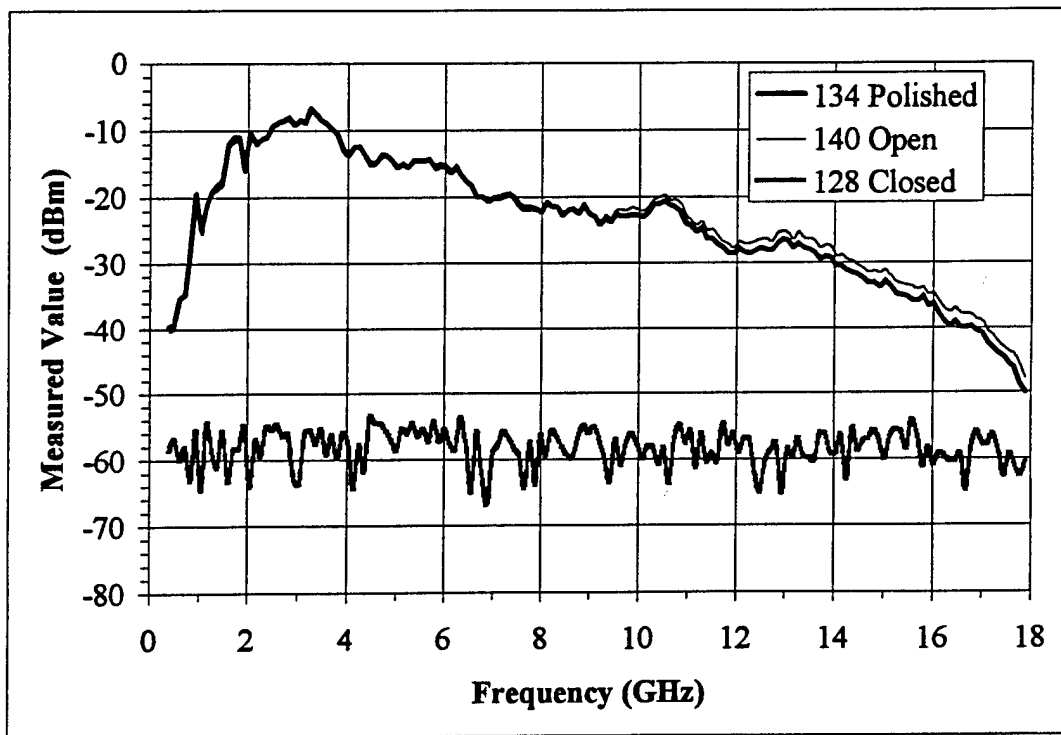
Polished Substrate with BLWGN and 100 MHz: Raw Data at 0° Incidence, 5'5"



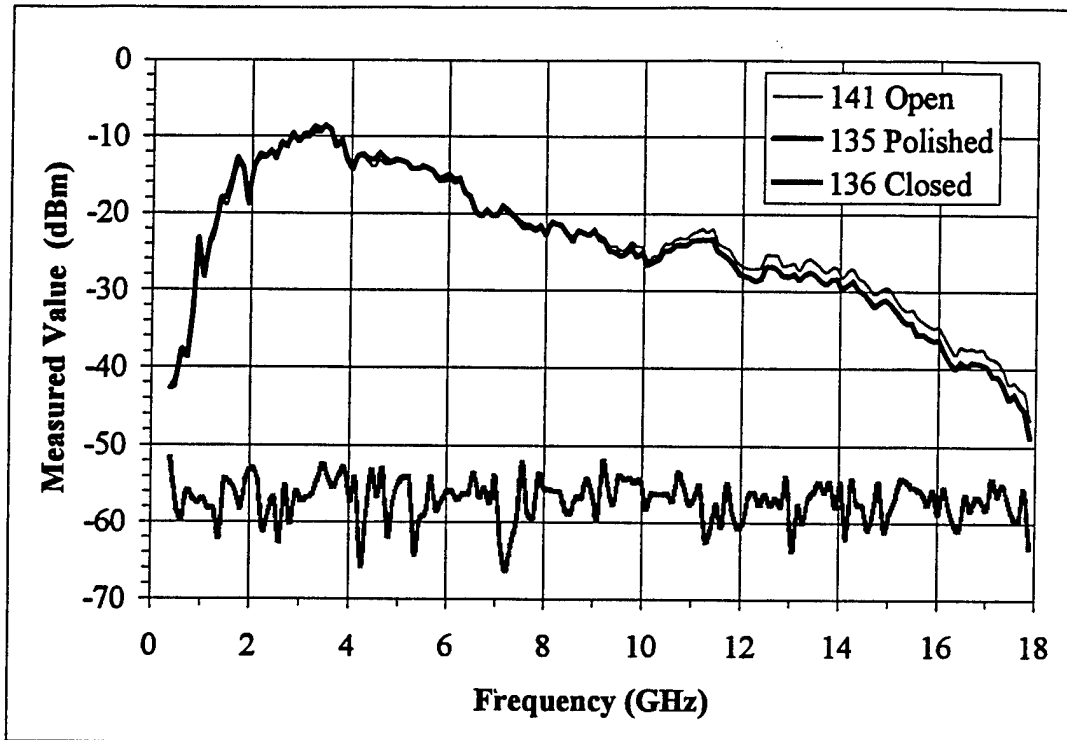
Polished Substrate with BLWGN and 100 MHz: SE at 0° Incidence, 5'5"



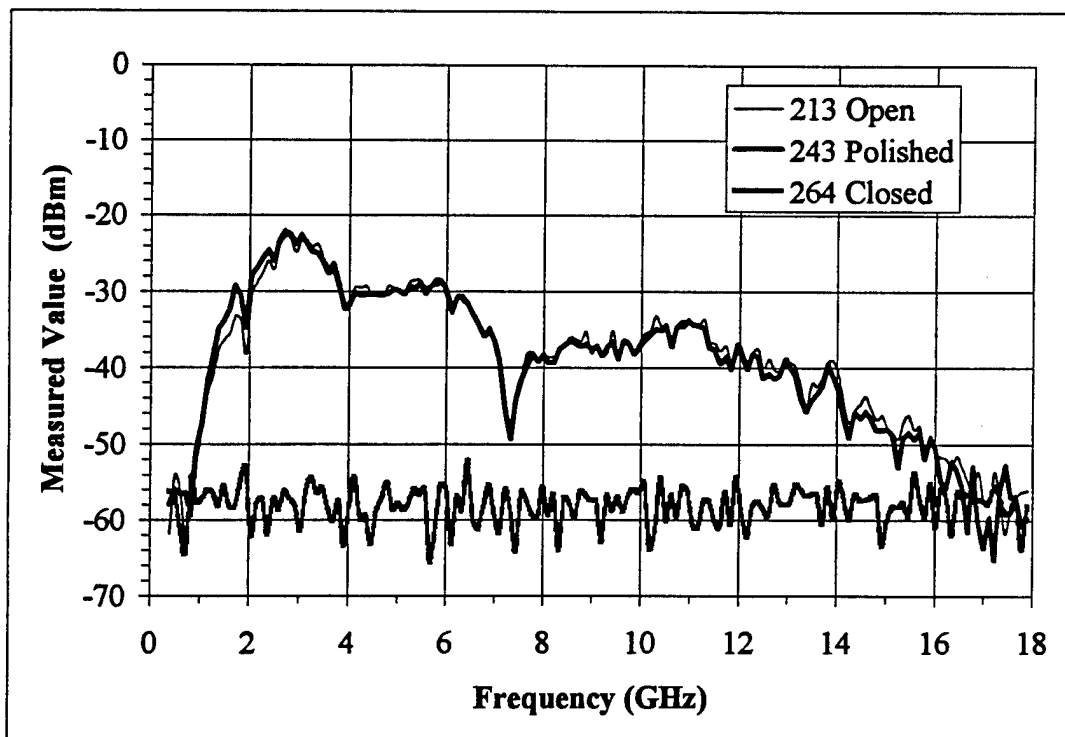
Polished Substrate in EMSC with 100 MHz: Open, Probe A, Closed



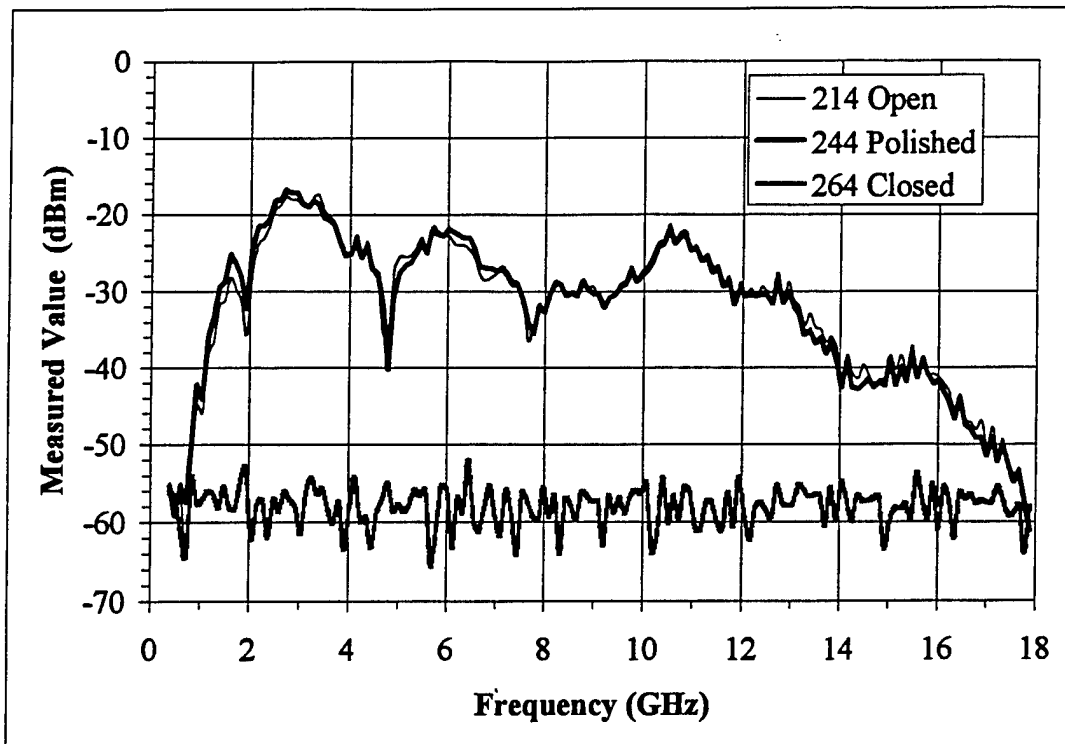
Polished Substrate in EMSC with 100 MHz: Open, Probe B, Closed



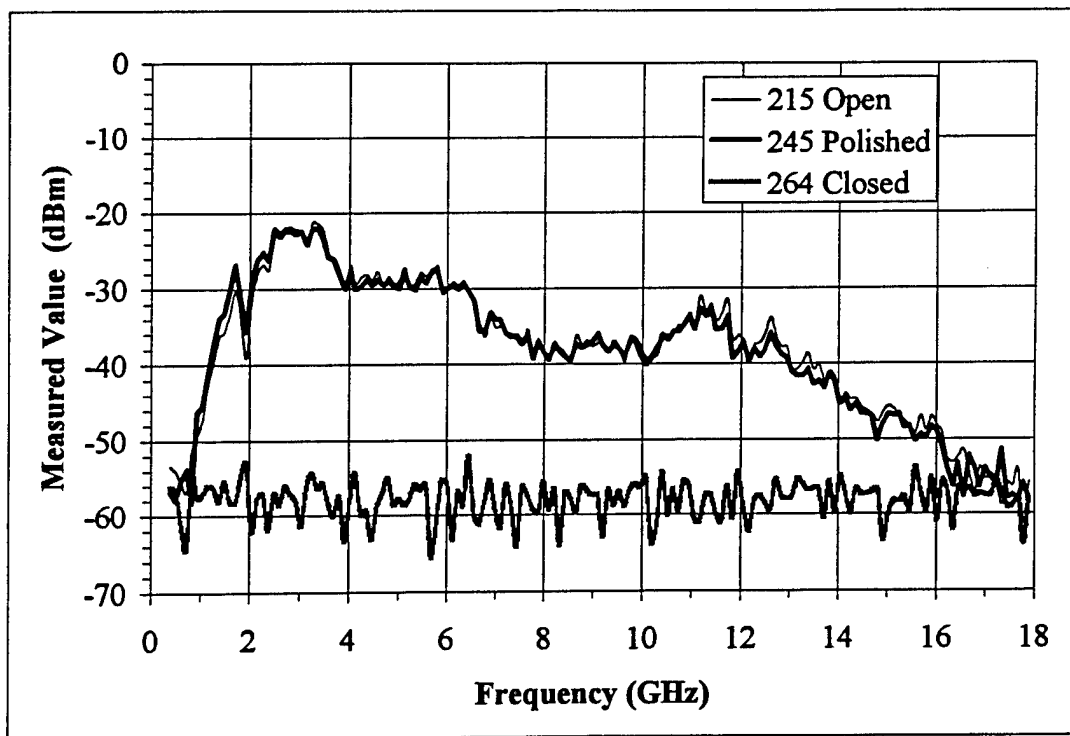
Polished Substrate in EMSC with 100 MHz: Open, Probe C, Closed



Polished Substrate with BLWGN and 100 MHz: Open, Probe A, Closed



Polished Substrate with BLWGN and 100 MHz: Open, Probe B, Closed



Polished Substrate with BLWGN and 100 MHz: Open, Probe C, Closed

DISTRIBUTION LIST

AUL/LSE Bldg 1405 - 600 Chennault Circle Maxwell AFB, AL 36112-6424	1 cy
DTIC/OCP 8725 John J. Kingman Rd, Suite 0944 Ft Belvoir, VA 22060-6218	2 cys
AFSAA/SAI 1580 Air Force Pentagon Washington, DC 20330-1580	1 cy
AFRL/PSOTL Kirtland AFB, NM 87117-5776	2 cys
AFRL/PSOTH Kirtland AFB, NM 87117-5776	1 cy
Sienna Technologies, Inc. 19501 144th Ave NE, Suite F-501 Woodinville, WA 98072	1 cy
Official Record Copy AFRL/DEPE/Hector Del Aguila	5 cys